

# A CLUSTER OF LOW-REDSHIFT LYMAN- $\alpha$ CLOUDS TOWARD PKS 2155-304. I. LIMITS ON METALS AND D/H

J. MICHAEL SHULL, STEVEN V. PENTON, JOHN T. STOCKE,  
AND MARK L. GIROUX

Center for Astrophysics and Space Astronomy,  
Department of Astrophysical and Planetary Sciences,  
University of Colorado, Campus Box 389, Boulder, CO 80309  
Electronic mail: mshull@casa.colorado.edu, spenton@casa.colorado.edu,  
stocke@casa.colorado.edu, giroux@casa.colorado.edu

J. H. VAN GORKOM AND YONG-HAN LEE  
Astronomy Department, Columbia University,  
538 W. 120<sup>th</sup> St., New York, NY 10027  
Electronic mail: jvangork@astro.columbia.edu

CHRIS CARILLI  
National Radio Astronomy Observatory,  
P.O. Box O, Socorro, NM 87801  
Electronic mail: ccarilli@aoc.nrao.edu

## ABSTRACT

We report observations from the *Hubble Space Telescope* (HST) and the VLA on the galactic environment, metallicity, and D/H in strong low-redshift Ly $\alpha$  absorption systems toward the bright BL Lac object PKS 2155-304. These studies are intended to clarify the origin and chemical evolution of gas at large distances from galaxies. With GHRS/G160M data at  $\sim 20$  km s $^{-1}$  resolution, we detect a total of 14 Ly $\alpha$  absorbers, six of them clustered between  $cz = 16,100$  and  $18,500$  km s $^{-1}$ . Although *ORFEUS* studies claimed Lyman continuum (Lyc) absorption at  $z \approx 0.056$  with  $N(\text{H I}) = (2 - 5) \times 10^{16}$  cm $^{-2}$ , the Ly $\alpha$  data suggest a range,  $N(\text{H I}) = (3 - 10) \times 10^{14}$  cm $^{-2}$ . Even higher columns, needed for consistency with the *ORFEUS* Lyc results, are possible if the Ly $\alpha$  line core at  $17,000 \pm 50$  km s $^{-1}$  contains narrow H I components. We identify the Ly $\alpha$  cluster with a group of five H I galaxies offset by  $(400 - 800)h_{75}^{-1}$  kpc from the sightline. The two strongest absorption features cover the same velocity range as the H I emission in the two galaxies closest to the line of sight. If the Ly $\alpha$  is associated with these galaxies, they must have huge halos ( $400 - 500h_{75}^{-1}$  kpc) of highly turbulent, mostly ionized gas. The Ly $\alpha$  absorption could also arise from an extended sheet of intragroup gas, or from smaller primordial clouds and halos of dwarf galaxies.

We see no absorption from Si III  $\lambda 1206$ , C IV  $\lambda 1548$ , or deuterium Ly $\alpha$  at the expected positions of the strongest Ly $\alpha$  absorbers. Photoionization models yield  $(4\sigma)$

limits of  $(\text{Si}/\text{H}) \leq 0.003(\text{Si}/\text{H})_{\odot}$ ,  $(\text{C}/\text{H}) \leq 0.005(\text{C}/\text{H})_{\odot}$ , and  $(\text{D}/\text{H}) \leq 2.8 \times 10^{-4}$  if  $\text{N}(\text{H I})$  has the *ORFEUS* value of  $2 \times 10^{16} \text{ cm}^{-2}$ . The limits increase to 0.023 solar metallicity and  $\text{D}/\text{H} \leq 2.8 \times 10^{-3}$  if  $\text{N}(\text{H I})$  is only  $2 \times 10^{15} \text{ cm}^{-2}$ . These limits can be improved with further studies by HST/STIS and measurements of the Ly $\gamma$  and higher Lyman series absorption by FUSE. However, the current data suggest that the intergalactic gas in this group has not been enriched to the levels suggested by X-ray studies of intracluster gas. Because of their low metallicity and large distance from galaxies, these absorbers could be primordial gas clouds.

*Subject headings:* cosmology: observations — galaxies: abundances — ISM: H I — quasars: absorption lines

## 1. INTRODUCTION

The origin of the low-redshift Ly $\alpha$  absorption clouds discovered by the *Hubble Space Telescope* (Bahcall et al. 1991; Morris et al. 1991; Stocke et al. 1995) remains a mystery, made more tantalizing by the possibility that they may contain significant mass. Are they remnants of the high-redshift Ly $\alpha$  forest, or are they associated with past episodes of star formation, galactic outflows, and galaxy interactions? Based on their frequency, estimated size, and an ionization correction, they appear to contain a substantial amount ( $\Omega_b \geq 0.003h_{75}^{-1}$ ) of dark baryons (Shull et al. 1996; Shull 1997). There are also strong indications that some of these absorbers are associated with galaxies (Lanzetta et al. 1995; Stocke et al. 1995; van Gorkom et al. 1996), although the distances to the nearest bright galaxies are often quite large (Morris et al. 1993; Stocke et al. 1995; Shull et al. 1996; Grogan & Geller 1998).

From numerical models, it now appears that the high- $z$  Ly $\alpha$  forest is part of a complicated gaseous structure, formed by the gravitational fluctuations of dark-matter potentials (Cen et al. 1994; Hernquist et al. 1996; Zhang et al. 1997) and at least partially “polluted” by heavy element nucleosynthesis during the epoch of galaxy formation. At high redshift, heavy elements (C IV, Si IV, C II) have been detected at  $\sim 10^{-2.5}$  times solar metallicity in 50–75% of the Ly $\alpha$  forest clouds above  $10^{14.5}$  cm $^{-2}$  column density (Cowie et al. 1995; Tytler 1995). From X-ray measurements of Fe-line strengths in galaxy clusters, Mushotzky & Loewenstein (1997) suggest that intragroup gas might be enriched to levels of 10% solar metallicity at  $z > 0.4$ . However, extrapolating these ideas to low redshift or to all Ly $\alpha$  clouds is difficult. Although a few metal-line absorption systems have been detected at moderate redshift, no low-redshift Ly $\alpha$ -only absorber has yet been examined for the presence of heavy elements, which would indicate contamination by star formation. To investigate this possibility in the Ly $\alpha$  forest requires finding absorbers of sufficient column density to detect metals [ $N(\text{H I}) > 10^{16}$  cm $^{-2}$ ] and located appropriately distant ( $D > 200$  kpc) from neighboring galaxies to suggest primordial gas.

We now believe to have found an ideal target and absorbers, based on our newly analyzed ultraviolet spectra of PKS 2155-304 from the *Hubble Space Telescope* (HST) and 21-cm emission images from the *Very Large Array* (VLA). Toward this bright, variable ( $V = 13.1 - 13.7$ ) BL Lac object, a strong Ly $\alpha$  line at  $cz \approx 17,000$  km s $^{-1}$  was initially identified by the IUE satellite (Maraschi et al. 1988). This and other Ly $\alpha$  lines were confirmed by low-resolution HST spectra with the Faint Object Spectrograph (FOS/G130H) (Allen et al. 1993) and with the Goddard High Resolution Spectrograph (GHRS/G140L) (Bruhweiler et al. 1993). The absorption was resolved by HST into at least two and possibly three systems. Using fits to Lyman-continuum (Lyc) absorption near 960–970 Å in low-resolution *ORFEUS* spectra, Appenzeller et al. (1995) claimed that the 17,000 km s $^{-1}$  absorbers had a combined column  $N(\text{H I}) \approx (2 - 5) \times 10^{16}$  cm $^{-2}$ . From our HST/GHRS measurements of the corresponding Ly $\alpha$  absorption, we estimate a range,  $N(\text{H I}) = (3 - 10) \times 10^{14}$  cm $^{-2}$ . Later in this paper, we will assess the accuracy of the H I column densities associated with the Lyc absorption and discuss the conditions under which the *ORFEUS* and HST measurements could be reconciled.

Previously, our group observed the PKS 2155-304 field with the VLA (van Gorkom et al. 1996) and found evidence for three H I galaxies corresponding to Ly $\alpha$  absorbers at  $cz = 5100$ , 16,500, and 17,000 km s $^{-1}$ . We associated the 17,000 km s $^{-1}$  absorbers with a small group of galaxies offset from the PKS 2155-304 sightline by  $(400 - 800)h_{75}^{-1}$  kpc for a Hubble constant  $H_0 = (75 \text{ km s}^{-1} \text{ Mpc}^{-1})h_{75}$ . In this paper, we combine new HST and VLA observations with theoretical interpretation of the PKS 2155-304 sightline, which is unusual in the large number of strong Ly $\alpha$  absorbers and their association with four large galaxies located within  $\sim 1$  Mpc. This number of galaxies would be high by chance, based upon the observed two-point correlation function. The average space density of galaxies in this local region,  $n_{\text{gal}} \sim 1 \text{ Mpc}^{-3}$ , is  $\sim 100$  times the large-scale average density of  $L_*$  galaxies (Marzke, Huchra & Geller 1994). This suggests the presence of a small group that has recently turned around from the Hubble flow, much like our Local Group. These galaxies probably have not undergone significant mergers, but the presence of strong, broad Ly $\alpha$  absorption from extended gas may indicate some dynamical interaction.

In § 2.1, we describe new HST/GHRS observations at 20 km s $^{-1}$  resolution between 1258 and 1293 Å ( $cz = 10,440 - 19,060 \text{ km s}^{-1}$ ). We detect 7 Ly $\alpha$  absorbers with equivalent widths ranging from 68 to 467 mÅ. We also reanalyze an archival GHRS/G160M spectrum at 1223 – 1258 Å ( $cz = 1809 - 10,446 \text{ km s}^{-1}$ ) and identify 7 definite Ly $\alpha$  absorbers (21–201 mÅ). In § 2.2, we present new VLA studies of H I emission in the 2155-304 field from  $cz = 16,283 - 17,571 \text{ km s}^{-1}$ , a velocity range that includes four Ly $\alpha$  absorption systems. In § 3, we discuss the results of these studies. The new VLA data provide accurate correspondence with the Ly $\alpha$  absorbers, suggesting that the absorption might arise from extended halos or intragroup gas over a region 1 Mpc in diameter that could total  $10^{11} - 10^{12} M_\odot$  in mass, if bound. The HST data also allow us to set limits on the metallicity of the strongest absorbers from the absence of Si III  $\lambda 1206$  and C IV  $\lambda 1548$ , and they provide a limit on D/H from residual (D I) Ly $\alpha$  absorption in the shortward wing of the strongest absorber. In § 4 we summarize our conclusions and give suggestions for further study. Somewhat contrary to the kinematic evidence, the low metallicities,  $[\text{Si}/\text{H}] \leq 0.003$  solar and  $[\text{C}/\text{H}] \leq 0.005$  solar, would suggest that some primordial gas may still reside amidst the large-scale filaments of galaxies.

## 2. OBSERVATIONS

### 2.1. New HST/GHRS Spectra

The target, PKS 2155-304, lies at redshift  $z = 0.116$  or  $cz = 34,775 \text{ km s}^{-1}$  (Falomo, Pesce & Treves 1993). It was observed by HST during Cycle 6 on October 5, 1996, using the GHRS with the G160M grating and post-COSTAR optics. The continuum flux near 1280 Å was  $(8.7 \pm 0.3) \times 10^{-14} \text{ ergs cm}^{-2} \text{ s}^{-1} \text{ Å}^{-1}$ , about 70% of the median flux for this object over the past 15 years of observations in the IUEAGN database (Penton, Shull & Edelson 1998). Over the interval 1258–1293 Å, we obtained a resolution of 4.5 km s $^{-1}$  per 0.018 Å quarter-stepped pixel or

$\sim 20$  km s $^{-1}$  per resolution element.

The wavelength scale was determined by assuming that the Galactic interstellar S II absorption features at 1250.584, 1253.811, and 1259.519 Å lie at zero velocity in the local standard of rest (LSR). Based on the Bell Labs 21-cm survey (Stark et al. 1992), the dominant H I absorption in this direction lies at  $V_{\text{LSR}} \approx V_{\text{hel}}$ , within the accuracy ( $\pm 2$  km s $^{-1}$ ) of the observations. This correction in the wavelength scale in the new data (Fig. 1) was +0.029 Å, and that in the archival data (Fig. 2) was –0.001 Å. Our observations correspond to redshifted velocities  $cz = 10,440 - 19,060$  km s $^{-1}$  ( $z = 0.035 - 0.064$ ) in the Ly $\alpha$  line. According to previous convention, we quote heliocentric velocities,  $cz$ , and compute expected line positions from  $\lambda = \lambda_0(1 + z)$ . We do not make relativistic corrections to the velocities.

Figure 1 shows our new GHRS/G160M data (1258–1293 Å) with  $\text{S/N} \approx 20$ . Figure 2 shows our reanalysis of an unpublished archival GHRS/G160M spectrum with  $\text{S/N} \approx 34$  (1223–1258 Å) taken with pre-COSTAR optics. The 17,000 km s $^{-1}$  Ly $\alpha$  absorbers are the strongest of the low-redshift ( $z < 0.1$ ) absorbers found in HST searches other than associated absorbers with  $z_{\text{abs}} \approx z_{\text{em}}$ . Because of the exceptional brightness of the background source ( $\sim 13$  mag) and the high H I column densities ( $\geq 10^{16}$  cm $^{-2}$ ), these absorbers are ideally suited for measuring heavy-element abundances in the low- $z$  forest. As of this writing, our group has studied  $\sim 100$  low-redshift Ly $\alpha$  absorbers toward 11 bright quasars and Seyfert galaxies (Stocke et al. 1995; Shull et al. 1996; Shull 1997) with more absorbers under analysis (Penton et al. 1998). Our goal is to understand the physical structure of these clouds and their possible connections with galaxy halos, large-scale structure, and voids. Our data reduction method was described in these earlier papers. Complete results on the seven targets in our HST Cycle 6 observations, together with calibration, are described in Penton et al. (1998).

The GHRS spectra were taken through the 2" large science aperture, using the standard quarter-diode sub-stepping pattern to yield pixels of 0.018 Å in FP-split mode. We recalibrated our spectra using IRAF/STSDAS/CALHRS and the final GHRS reference files (Sherbert & Hulbert 1997) with polynomial background subtraction. One noteworthy point concerns our treatment of the HST/GHRS error vectors, which affect how we gauge the statistical significance of weak features. We found that the error vectors produced by the IRAF/STSDAS program **specalign** in the HST Data Handbook do not agree with those obtained by standard propagation of errors from individual subexposures. We have therefore chosen to perform our own error propagation and spectral coaddition using the IDL software package. Spectral coaddition was weighted by exposure time on a quarter-stepped, pixel-by-pixel basis, removing blemished pixels. This procedure gives some pixels less exposure time than others, but it prevents photocathode blemishes from being erroneously flagged as absorption features. In some cases, this procedure results in no exposure time being available for some pixels; straight lines between the last known good flux values are then used in Figures 1 and 2.

The significance of the detected lines (in  $\sigma$ ) is defined as the integrated S/N per resolution

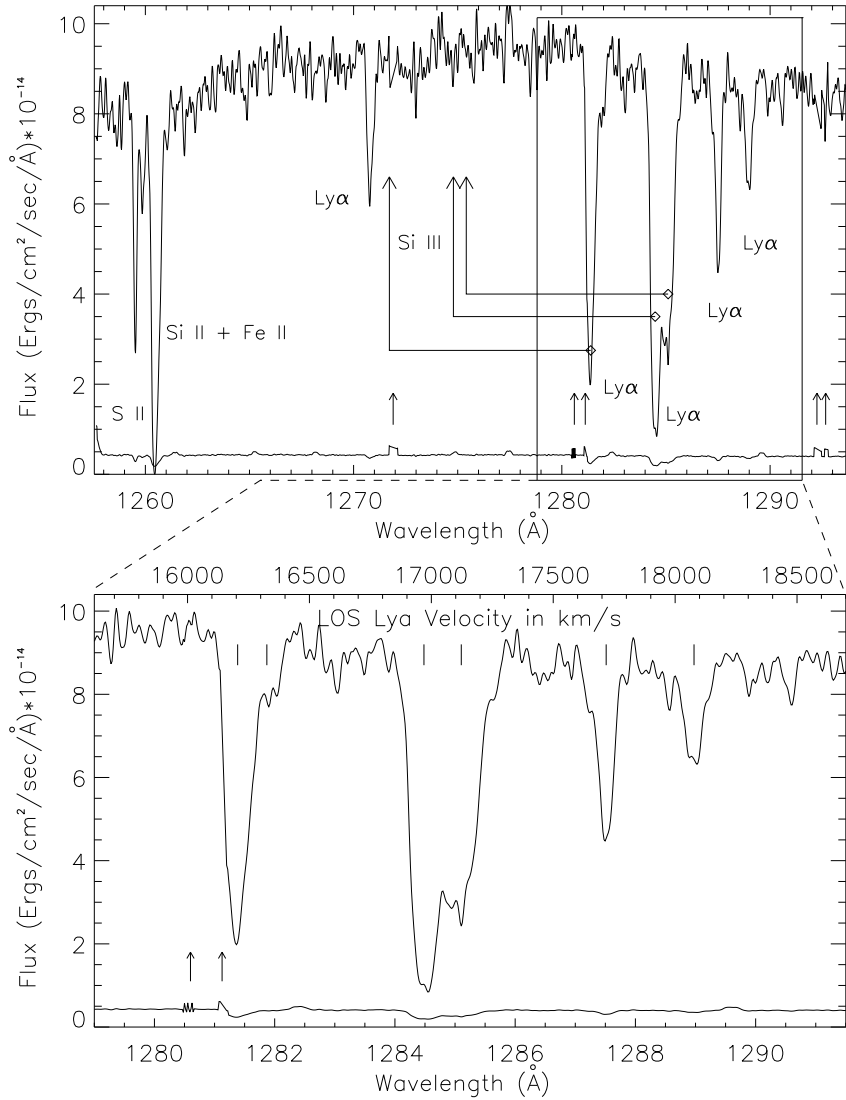


Fig. 1.— **Top:** Smoothed HST/GHRS (G160M) spectrum of PKS 2155-304 shows multiple Ly $\alpha$  absorption systems, with several strong absorbers at  $cz \approx 17,000 \text{ km s}^{-1}$ . Because of smoothing, the absorbers do not reach zero flux; error vector ( $1\sigma$ ) is shown at base. Small arrows near error vector show deleted photocathode blemishes. Lines at 1259–1261 Å are Galactic interstellar absorption; the weak line at 1259.869 Å is Si II in a high-velocity cloud at  $V \approx -132 \text{ km s}^{-1}$ . Upper limits on Si III  $\lambda 1206.50$  absorption at 1274.7 Å and 1275.2 Å (see arrows) correspond to  $[\text{Si}/\text{H}] < 0.003$  solar abundance ( $4\sigma$ ). **Bottom:** Six Ly $\alpha$  absorbers ( $cz = 16,120 - 18,590 \text{ km s}^{-1}$ ) including strong features near 1281 and 1285 Å, estimated to have total  $N(\text{H I}) = (2 - 5) \times 10^{16} \text{ cm}^{-2}$  from Ly $\alpha$  absorption (Appenzeller et al. 1995).

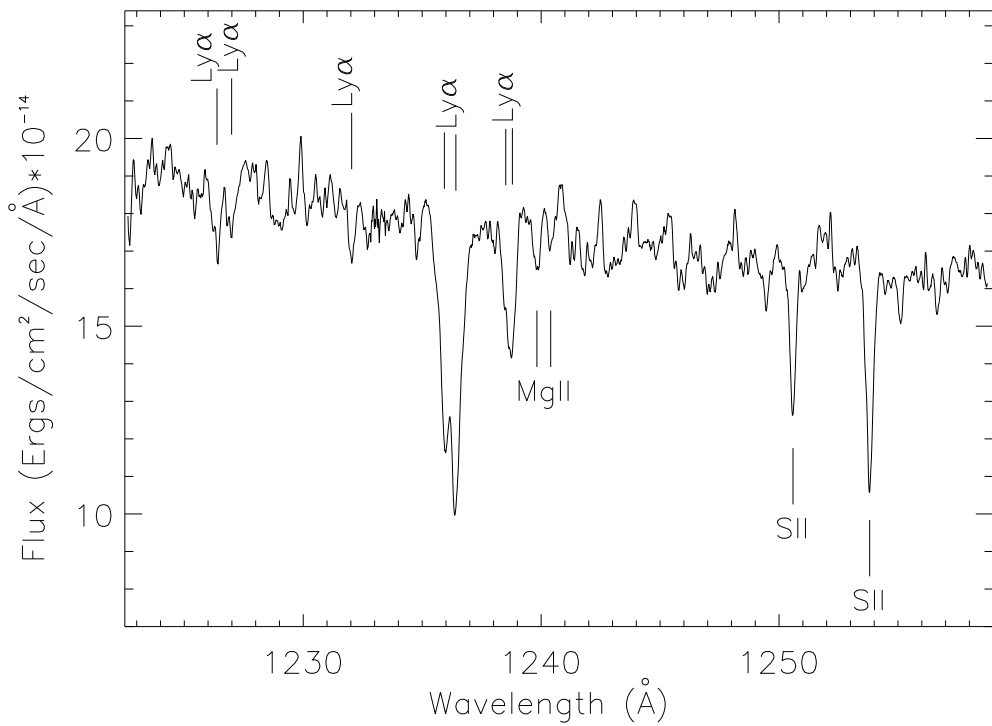


Fig. 2.— Reanalyzed archival GHRS/G160M spectrum from 1223 – 1258 Å shows 7 Ly $\alpha$  lines and Galactic interstellar lines of S II (1250.584, 1253.811 Å) and Mg II (1239.925, 1240.395 Å). The Ly $\alpha$  feature near 1236 Å consists of two components separated by 122 km s<sup>-1</sup> at comparable velocity to an H I galaxy at  $cz \approx 5100$  km s<sup>-1</sup> (van Gorkom et al. 1996). We identify the blended absorbers at 1238.426 and 1238.744 Å as Ly $\alpha$ , despite their proximity to Galactic N V (see text).

element of the fitted absorption feature. The status of “definite absorber” is given to features greater than  $4\sigma$  significance (Penton et al. 1998). Table 1 lists the identified absorption features and their equivalent widths. We see the expected Galactic interstellar lines of S II  $\lambda 1259.519$  and Si II  $\lambda 1260.422$ , as well as a high-velocity cloud in Si II at  $V_{\text{LSR}} = -132 \text{ km s}^{-1}$ , which was also seen in C IV at  $V_{\text{LSR}} = -141 \pm 9 \text{ km s}^{-1}$  by Sembach et al. (1998). We also confirm the strong intergalactic Ly $\alpha$  absorbers near  $17,000 \text{ km s}^{-1}$ . A blowup of the  $1278\text{--}1292 \text{ \AA}$  region shows that many of the Ly $\alpha$  lines have velocity substructure, which we model as separate Gaussian components. We included these additional components to reduce the  $\chi^2$  per degree of freedom whenever the resulting components were above  $4\sigma$  significance. In no case did we allow more than two components per blended absorption feature, although we occasionally tested for three.

In addition to the definite Ly $\alpha$  absorbers, we found a number of features at the  $3 - 4\sigma$  level that might be verified with future STIS data. Examples of these “possible features” occur at  $1229.0$ ,  $1243.2$ ,  $1249.5$ ,  $1264.8$ ,  $1286.45$ , and  $1290.58 \text{ \AA}$ . The local continua are uncertain near these features, and some of the features are too broad ( $\geq 120 \text{ km s}^{-1}$ ) to be discrete Ly $\alpha$  absorbers by our criteria. In these cases, we have decided to be conservative and not classify them as definite.

We also analyzed an archival spectrum (Fig. 2) taken with the GHRS/G160M using pre-COSTAR optics. This spectrum was reduced and analyzed in a manner identical to that in Figure 1, with the wavelength scale zero point set to the LSR using the Galactic interstellar S II lines at  $1250.584$  and  $1253.811 \text{ \AA}$ . Between  $1223$  and  $1258 \text{ \AA}$ , we detect 7 definite Ly $\alpha$  lines and three Galactic interstellar lines: the two S II resonance lines and the weak Mg II doublet.

The strong Ly $\alpha$  feature at  $1236 \text{ \AA}$  is easily detected and is resolved into two subcomponents separated by  $122 \text{ km s}^{-1}$ . This pair of lines, at  $cz = 4999$  and  $5121 \text{ km s}^{-1}$ , lies at the same velocity as the H I detected galaxy at  $21^{\text{h}} 57^{\text{m}} 04^{\text{s}}$ ,  $-30^{\circ} 25.5$  just off the eastern edge of Figure 3 and discussed in detail by van Gorkom et al. (1996). This sub- $L_*$  galaxy is located  $\sim 300h_{75}^{-1} \text{ kpc}$  from the PKS 2155-304 sightline. The absorption line at  $1238.744 \text{ \AA}$  lies  $0.077 \text{ \AA}$  blueward of the expected position of Galactic N V  $\lambda 1238.821$ . We identify this line as Ly $\alpha$  because of the slight wavelength offset and what would be an unusual strength for N V. Based on the absence of the weaker line of the N V doublet at  $1242.804 \text{ \AA}$ , we believe that N V  $\lambda 1238.821$  contributes at most 30% (at the  $4\sigma$  level) to the equivalent width of the Ly $\alpha$  feature at  $1238.744 \text{ \AA}$ .

The PKS 2155-304 sightline appears to be unusual, both in the number of Ly $\alpha$  absorbers and in their strength. In total, from  $1223 - 1293 \text{ \AA}$ , we identify 14 Ly $\alpha$  absorbers with significance greater than  $4\sigma$ . With a correction for regions blocked by Galactic S II and Si II, these 14 Ly $\alpha$  absorbers correspond to an uncorrected frequency  $dN/dz = 250$  above  $21 \text{ m\AA}$  ( $N_{\text{HI}} \geq 10^{12.6} \text{ cm}^{-2}$ ), for  $N_{\text{HI}} \geq 10^{13} \text{ cm}^{-2}$ . This frequency is somewhat higher than the mean value, to similar absorption strength, in sightlines studied with the GHRS during cycles 2 and 4 (Shull et al. 1996). Probably the most unusual aspect of this sightline, however, is the large number of strong Ly $\alpha$  absorbers near  $17,000 \text{ km s}^{-1}$ . The strong correspondence in recession velocity between these Ly $\alpha$  absorbers and the surrounding galaxies argues that these clouds are not ejected from the

BL Lac object. Rather, they appear to be intervening clouds at distances given by the Hubble law,  $d \approx (227 \text{ Mpc})(V/17,000 \text{ km s}^{-1})h_{75}^{-1}$ , as we assume throughout this paper.

## 2.2. Deep VLA H I Imaging

Our previous results (van Gorkom et al. 1996) showed that two of the strongest Ly $\alpha$  absorbers found toward PKS 2155-304 at 17,100 km s $^{-1}$  are located within a loose group of galaxies. Three galaxies were detected in H I, two at the velocities of the absorbers, but no individual galaxy could be identified as being *associated* with the absorber. The high column densities observed in the absorbers suggested that there may be an extended component of intergalactic neutral gas. Column densities  $N(\text{H I}) < 10^{19} \text{ cm}^{-2}$  are rarely detected in emission (van Gorkom 1993), and common lore suggests that it may be ionized by the intergalactic UV background. The Ly $\alpha$  results suggested that this group may be the ideal place to look for diffuse H I at very low column densities. We therefore reobserved the group in hope of detecting a low surface brightness diffuse H I component.

The observations were made in 1996 May with the VLA in the 1 km (D) array with an extended north arm (3 km) to compensate for the low declination of the source. The total integration time was 40 hrs spread over 8 different runs. All observations were centered at the radio position of PKS 2155-304,  $21^{\text{h}} 55^{\text{m}} 58.30^{\text{s}}$ ,  $-30^{\circ} 27' 54.4''$  (B1950). We used a total bandwidth of 6.25 MHz centered at 16,880 km s $^{-1}$ ; the usable velocity range is about 1300 km s $^{-1}$ . On-line Hanning smoothing was employed, after which every other channel was discarded, leaving a set of 31 independent channels and resulting in a velocity resolution of 46 km s $^{-1}$ . The BL Lac object is a radio continuum source with a variable flux density. We measured a flux density of 0.45 Jy at 1.4 GHz. Extreme care was taken to properly calibrate the bandpass. Every 25 minutes a bandpass calibration was done, and the bandpass solution for these individual scans was interpolated to do the correction. As a result, our observations are limited by noise rather than by spectral dynamic range, which is better than 3000:1.

The U-V data for each of the 8 days were calibrated independently and inspected for interference and residual calibration errors. Subsequently, the U-V data of all runs were combined. The continuum was subtracted by making a linear fit in frequency to the calibrated complex visibilities of the line free channels (2-5 and 23-25). The resulting data were clipped at a level of 0.7 Jy to remove man-made and solar interference. Images were made using a taper that compromised between optimal surface brightness sensitivity and maximal sidelobe suppression (using the task IMAGR in AIPS, with robustness factor 1), resulting in a synthesized beam of  $54.4'' \times 38.6''$ . The rms noise in the channel images is  $0.15 \text{ mJy beam}^{-1}$ . The instrumental parameters are summarized in Table 2.

To search for H I, we imaged the entire primary beam ( $1^{\circ} \times 1^{\circ}$ ). To calculate H I masses, we use the luminosity distance (Sandage 1975) assuming that the group is at  $z = 0.057$  and using

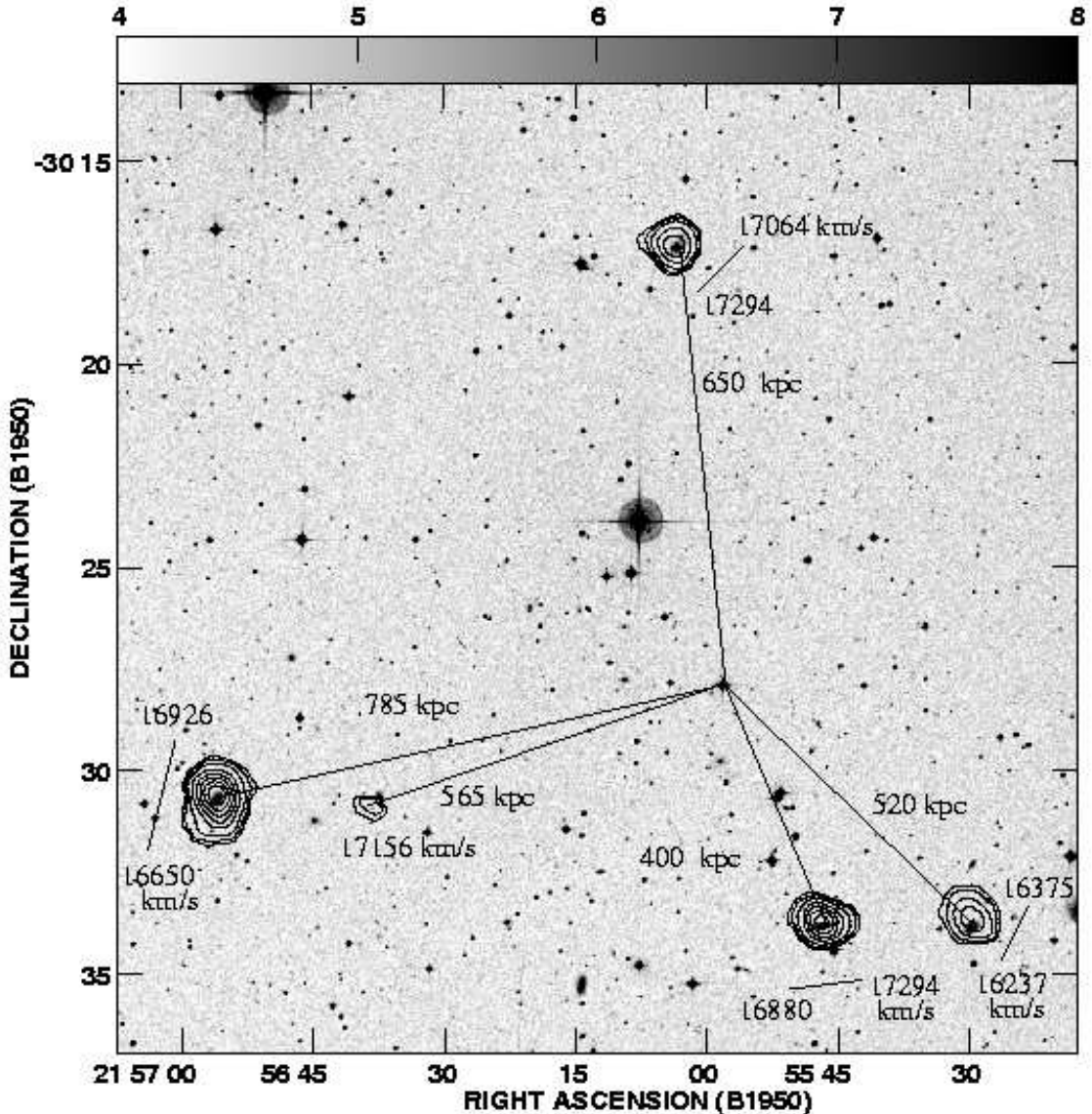


Fig. 3.— An overlay of the total H I emission (contours) toward PKS 2155-304 in the velocity range (16,283 – 17,571 km s<sup>-1</sup>) on an image of the digitized POSS. Five galaxies are detected in H I at projected distances from the sightline toward PKS 2155-304 of (400–785) $h_{75}^{-1}$  kpc. Contours levels are 1.65, 3.3, 6.6, 13.2, 19.8, 26.4, 33.0, 39.6  $\times 10^{19}$  cm<sup>-2</sup>. The image has been corrected for the primary beam response. Projected distances from the sight line are indicated in  $h_{75}^{-1}$  kpc. For each of the galaxies, the velocity range and approximate major axis of the H I emission are indicated. Note that the galaxy closest to the sightline covers in H I emission exactly the same velocity range as the broad Ly $\alpha$  absorption seen near 17,000 km s<sup>-1</sup>. The galaxy to the southwest covers about the same velocity range as the absorption feature near 16,200 km s<sup>-1</sup>.

$H_0 = 75h_{75}$  km s $^{-1}$  Mpc $^{-1}$  and  $q_0 = 0.5$ . Our  $6\sigma$  H I mass limit in the center of the field is  $(5 \times 10^8 M_\odot)h_{75}^{-2}$ . At full resolution, the column density sensitivity is  $2 \times 10^{19}$  cm $^{-2}$  ( $5\sigma$  over 57 kpc  $\times$  34 kpc  $\times$  46 km s $^{-1}$ ). The data were smoothed spatially and in velocity down to a resolution  $2' \times 3'$ , resulting in a detection limit of  $4 \times 10^{18}$  cm $^{-2}$  ( $5\sigma$  over 126 kpc  $\times$  189 kpc  $\times$  92 km s $^{-1}$ ). Owing to a lack of short spacings, the observations are much less sensitive to H I emission that is completely smooth on scales larger than  $15'$  in a single 46 km s $^{-1}$  velocity channel. These values are valid for the center of the field. Farther from the center, they have to be corrected for the change in primary beam response. The primary beam pattern is roughly gaussian with a FWHM of  $30'$ , and the limits are a factor two worse  $15'$  from the field center.

The properties of the five galaxies detected in H I are summarized in Table 3 and shown in Figure 3. Perhaps the most interesting result of these observations is what we do not find. We do not detect a faint intergalactic component in H I, nor do we detect any diffuse extended H I associated with the galaxies. Compared to van Gorkom et al. (1996), our new data are of much better quality and only show more clearly that the H I emission is confined to the galaxies at column densities well above  $10^{19}$  cm $^{-2}$ . In addition to the 3 galaxies detected in the previous observations, we detect to the southwest an S0 galaxy cataloged in the APM catalog (Loveday 1996) with a velocity range partly outside our band. We see H I to the northwest at 16,375 km s $^{-1}$ , moving toward the center of the galaxy at lower velocities. The lowest velocity where we have usable, though very noisy data, is at 16237 km s $^{-1}$ . Since this emission peaks only slightly to the northwest of the center, we infer that the systemic velocity of the galaxy must be about 16200 km s $^{-1}$ . This galaxy was not detected in our previous observations, because in those data that velocity range was seriously affected by interference.

The other new detection is a tiny dwarf galaxy to the east at 17,156 km s $^{-1}$ . In the current data, the galaxy only shows up in one channel, but at the  $8\sigma$  level. Going back to our previous data, we found the dwarf just above the noise in our oldest data set (and at the edge of the band there). Those data were taken with 11 km s $^{-1}$  velocity resolution, and the emission seems to cover about 60 km s $^{-1}$ . An overlay of just the dwarf on the digitized POSS is shown in Figure 4. A hint of some faint light ( $m_B = 22 \pm 0.5$ ) can be seen on the blue POSS image, but it is clear from the image that similar dwarfs could easily be missed optically. In H I the dwarf is just above our detection limit. Although somewhat brighter galaxies with larger H I masses could have been detected closer to the sightline, in fact none was seen (Fig. 3).

Are we getting any closer to identifying galaxies associated with the Ly $\alpha$  absorption? There are 3 galaxies with H I emission in the range 16,900 – 17,100 km s $^{-1}$ , the velocity of the deepest Ly $\alpha$  absorption. Thus, in the first instance, it is not obvious that the absorption would be *associated* with any one of the galaxies. In our previous work (van Gorkom et al. 1996) we noticed a curious phenomenon: in all cases, the Ly $\alpha$  absorption was at the systemic velocity of the closest galaxy. In the current, much improved, Ly $\alpha$  data we notice something even more curious: the two strong features at 17,100 km s $^{-1}$  and at 16,200 km s $^{-1}$  cover exactly the same velocity range as the H I emission in the two nearest galaxies. In Figure 3 we show the total H I

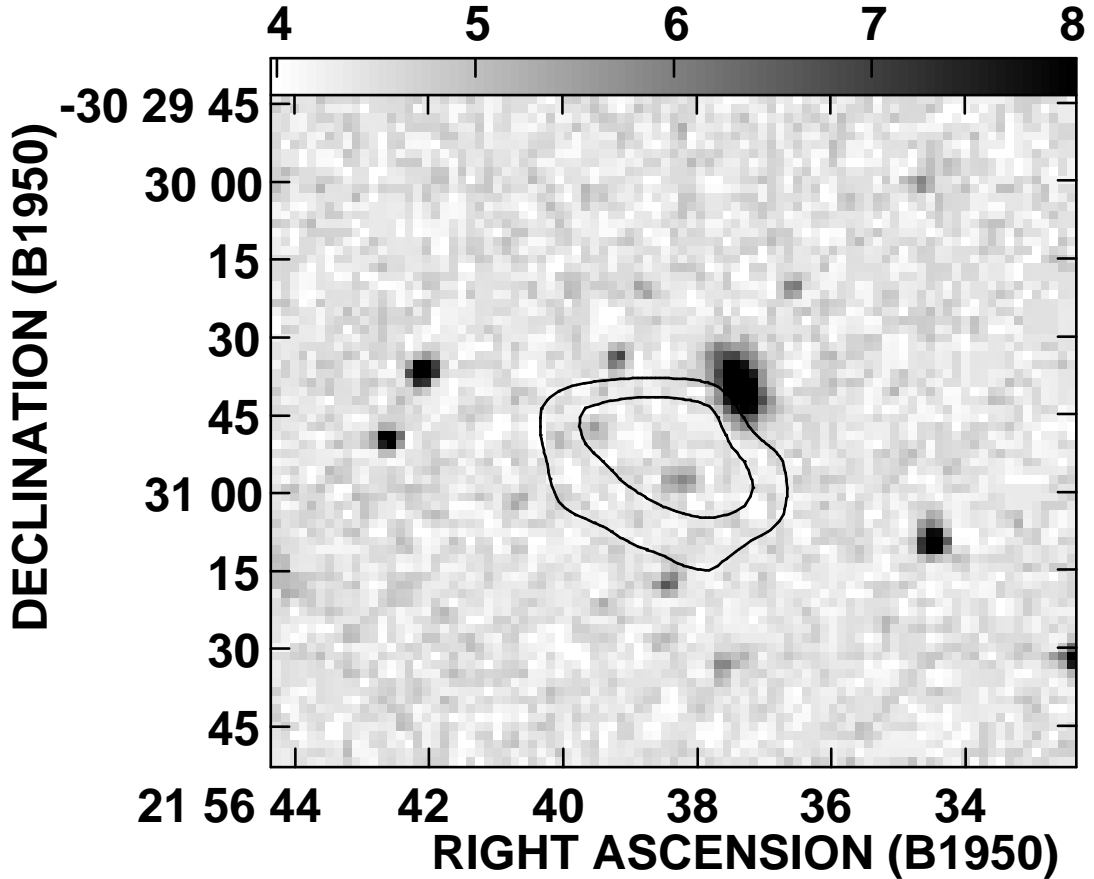


Fig. 4.— Overlay on the POSS of the dwarf galaxy to the east of PKS 2155-304 sightline at  $17,156 \text{ km s}^{-1}$ . Contours are same as in Fig. 3. This galaxy has an estimated blue magnitude  $m_B = 22 \pm 0.5$ . At the observed redshift distance,  $230h_{75}^{-1} \text{ Mpc}$ , its absolute magnitude is  $M_B \approx -15$ , or  $L \approx 0.014L_B^*$ .

emission contours overlaid on an optical image (greyscale), and we also indicate for each galaxy the sense of rotation and velocity extent of the H I emission. As in our previous data, there is no evidence for Ly $\alpha$  corotating with the H I disks. The broad widths of the Ly $\alpha$  absorbers in the current data is intriguing. It seems unlikely that the two strong absorbers are associated with their nearest galaxies only. If the width of the Ly $\alpha$  lines were to reflect the potential of the nearest galaxies, each would have a halo characterized by a flat rotation curve extending out to 400 and 500 kpc respectively. Perhaps more likely, the widths could indicate that the clouds probe a group potential. In that scenario we may be viewing two groups along the line of sight, one centered at 17,100 km s $^{-1}$ , the other at 16,200 km s $^{-1}$ . The detection of 3 galaxies with systemic velocities close to 17,100 km s $^{-1}$  makes it plausible that there is indeed a loose group at this velocity. Our velocity coverage does not extend to sufficiently low velocities to make any statements about the presence of a group at 16,200 km s $^{-1}$ .

### 3. RESULTS AND DISCUSSION

#### 3.1. Extended Halo and Intragroup Gas

The combined HST and VLA data suggest that the 17,000 km s $^{-1}$  Ly $\alpha$  absorption lines arise in a group environment. Between 16,100 and 18,100 km s $^{-1}$ , we observe 6 Ly $\alpha$  absorbers and four large (VLA) galaxies at similar velocities. The velocity centroid and radial velocity dispersion of the four galaxies are  $\langle V_{\text{gal}} \rangle = 16,853$  km s $^{-1}$  and  $\sigma_{\text{gal}} = 325$  km s $^{-1}$ . The equivalent statistics for the 6 Ly $\alpha$  absorbers are  $\langle V_{Ly} \rangle = 17,070$  km s $^{-1}$  and  $\sigma_{Ly} = 740$  km s $^{-1}$ . The fact that the strongest Ly $\alpha$  absorbers (1284.484 Å and 1285.097 Å) lie close to  $\langle V_{Ly} \rangle$  suggests that the center of the gravitational potential well may be centered at  $V \approx 17,000$  km s $^{-1}$ . Before we interpret the larger velocity dispersion of Ly $\alpha$  lines, it is worth noting that this galaxy group was observed in H I emission with the VLA over a more limited velocity range (16,283 – 17,571 km s $^{-1}$ ) than the Ly $\alpha$  lines.

The simplest interpretation of the data is that the absorbing gas arises in intragroup material stripped or blown out of the gas-rich galaxies. However, there is no direct evidence for this interpretation in the H I emission data. Nor are galaxy H I halos expected to be this dense at such enormous radii (Dove & Shull 1994). Combining the 740 km s $^{-1}$  velocity dispersion of the 6 definite Ly $\alpha$  absorbers with the mean projected separation,  $\langle R \rangle \approx 1.0$  Mpc between the four galaxies, we obtain a virial mass estimate,

$$M_{\text{vir}} \approx \frac{3\sigma_r^2 \langle R \rangle}{2G} \approx (2 \times 10^{14} M_{\odot}) h_{75}^{-1}. \quad (1)$$

The estimated velocity dispersion and size/mass scale are those of a modest group, less than the size of the Virgo cluster. The mean distance of these galaxies at  $\langle V_{\text{gal}} \rangle = 16,853$  km s $^{-1}$  is  $225 h_{75}^{-1}$  Mpc or  $(m - M) = 36.8$ . The break in the standard luminosity function is  $L_* = (9 \times 10^9 L_{\odot}) h_{75}^{-2}$  or  $M_* = -19.4 + 5 \log h_{75}$  (Marzke et al. 1994) in the Zwicky (blue) magnitude system. Thus, an

$L_*$  galaxy in this group would lie at  $m_B \approx 17.4$ . Using two slightly brighter galaxies in the field for calibration of the SRC-J plate magnitudes (Lauberts & Valentijn 1989), we have estimated  $B_0$  magnitudes for the five galaxies around PKS 2155-304. In terms of  $L_*$ , they are: north ( $0.3L_*$ ), east ( $0.9L_*$ ), south ( $1.4L_*$ ), southwest ( $3.0L_*$ ), and dwarf ( $0.014L_*$ ). Thus, three of the H I galaxies have luminosities essentially at or above  $L_*$ .

Although drawing statistical inferences from only four galaxies is risky, we have attempted to estimate the possible number of fainter galaxies, both observationally and theoretically. In a CFHT image (Wurtz et al. 1997) centered on PKS 2155-304, of radius  $160h_{75}^{-1}$  kpc at  $cz = 17,000$  km s $^{-1}$ , we found five galaxies in excess of the background to a limit of  $m_B \approx 21$ , about 3.5 magnitudes below  $L_*$ . Over the larger field of  $600h_{75}^{-1}$  kpc radius, defined by the four H I galaxies, this corresponds to  $\sim 60$  excess galaxies. However, this photometry does not constrain the redshift of these excess galaxies; most, if not all, could lie at the redshift,  $z_{\text{em}} = 0.116$ , of PKS 2155-304 (Falomo et al. 1993). Since BL Lac objects are routinely found in poor clusters (Wurtz et al. 1997), these five excess galaxies are likely to be associated with PKS 2155-304.

If we integrate a Schechter luminosity function,  $\phi(L) = \phi_*(L/L_*)^{-1} \exp(-L/L_*)$ , down to  $0.04L_*$  ( $m_B \approx 21$ ), we would expect between 3 and 10 times more galaxies, compared to those above  $0.3L_*$  and  $0.9L_*$ , respectively. Scaling from the observed H I galaxies above those limits, we would expect to find between 10 and 30 galaxies associated with this group, down to  $0.04L_*$ . Therefore our preliminary optical survey is consistent with these expectations. However, since our radio H I survey detected only one dwarf galaxy in the field, gas-rich dwarfs may be scarce in this group. We are conducting a spectroscopic survey of the PKS 2155-304 field down to  $m_B \approx 19$  to test our hypothesis that the large VLA galaxies are accompanied by smaller galaxies, some closer to the PKS 2155-304 sightline.

We also investigated the possibility that hot gas associated with the strong absorbers at  $17,100$  km s $^{-1}$  might be responsible for the 600 eV absorption feature seen by the objective grating spectrometer on the *Einstein Observatory* (Canizares & Kruper 1984) and by the BBXRT spectrograph (Madejski et al. 1998). This possibility would only work if the X-ray absorption arose from an O V K-edge (626 eV rest frame, 592 eV observed) or an O VIII K $\alpha$  line (653 eV rest frame, 618 eV observed). We can rule out the O V hypothesis ( $T \approx 2 \times 10^5$  K) because it would require an unreasonably large hydrogen column,  $N_H = (1.7 \times 10^{22} \text{ cm}^{-2})\zeta_O^{-1}$ , for oxygen metallicity  $\zeta_O$ , in order to produce the observed optical depth,  $\tau \approx 2.5$ . The resulting gas densities would be quite high, across a 300 kpc slab, and the cooling time would be less than  $10^5$  yrs. Line absorption by O VIII would be more feasible, requiring a column density  $N_H \approx (1.3 \times 10^{19} \text{ cm}^{-2})\zeta_O^{-1}$ . However, neither of these cluster hot-gas models would explain the observed broad ( $\sim 30,000$  km s $^{-1}$ ) absorption widths. We conclude that the 600 eV absorption must be produced elsewhere, probably within PKS 2155-304.

Because the four bright galaxies are H I-rich spirals, it is also possible that these galaxies are not bound, based upon recent spectroscopic work on similar galaxy groups (Mulchaey & Zabludoff

1998; Zabludoff & Mulchaey 1998). Even if they are bound, these galaxies may not have virialized or closely interacted. If this is the case, the Ly $\alpha$  clouds may also be non-virialized, and our estimate of  $M_{\text{vir}}$  would be too large. This interpretation suggests that these clouds are portions of the gaseous filament out of which these spiral galaxies formed. If these clouds and galaxies are portions of a bound group, then we would expect the clouds to have metallicities of 0.1 – 0.3 solar, similar to the stripped and virialized gas in rich clusters and elliptical-rich groups (Mushotzky & Loewenstein 1997). In the unbound case, not only would X-ray emission be unlikely, but the metallicity of the gas would be substantially lower than 10% solar (see § 3.2).

In our earlier papers on the environments of the low- $z$  absorbers (Shull et al. 1996; van Gorkom et al. 1996), we estimated a space density,  $\phi_0 \approx (0.7 \text{ Mpc}^{-3})R_{100}^{-2}h_{75}$ , of low- $z$  Ly $\alpha$  clouds with  $N(\text{H I}) \geq 10^{13} \text{ cm}^{-2}$  and characteristic size scale  $(100 \text{ kpc})R_{100}$ , in order to explain their frequency per unit redshift. This space density is  $\sim 40$  times larger than that of  $L_*$  galaxies, but comparable to that of dwarf galaxies with  $L \approx 0.01L_*$ , suggesting a possible connection. However, the H I absorption cross sections of these dwarfs are uncertain, and it is unclear whether the extended gas was stripped out, blown out, or existed primordially.

The main results of our comparison between the Ly $\alpha$  absorption and the 21-cm emission can be summarized as follows: (1) 21-cm emission has been detected in this region, spread over 1 Mpc of sky and 1300 km s $^{-1}$  of velocity; (2) the large distances to the nearest bright galaxies ( $400\text{--}800h_{75}^{-1}$  kpc); and (3) the agreement in velocity (within  $\pm 100 \text{ km s}^{-1}$ ) between several of the Ly $\alpha$  absorbers and the H I galaxies to the south, southwest, and north. The proper interpretation of the Ly $\alpha$  absorbers toward PKS 2155-304 hinges on several geometrical issues. Does the Ly $\alpha$  absorption occur in a smoothly distributed layer, 200-600 kpc in depth, or in smaller, denser clumps? Some evidence for the latter interpretation comes from the fact that the Ly $\alpha$  absorption occurs in discrete systems in velocity space. Less certain is whether the absorbers are kinematically associated with the large galaxies. Although a single sight line through the region is not necessarily typical, the VLA observations suggest that the absorbing gas is distributed across a region  $\sim 1$  Mpc in diameter. As a first approximation, we will model the absorption as a homogeneous slab. We then explore more complex distributions, either in intergalactic clouds or in dwarf-galaxy halos.

In the homogeneous approximation, the total mass of gas in the vicinity of the cluster of galaxies around PKS 2155-304 can be estimated by assuming a slab of radius 500 kpc, depth  $D = 400$  kpc, mean column density  $N(\text{H I}) = 2 \times 10^{16} \text{ cm}^{-2}$ , exposed to an ionizing radiation field with specific intensity  $I_0 = 10^{-23} \text{ ergs cm}^{-2} \text{ s}^{-1} \text{ Hz}^{-1} \text{ sr}^{-1}$  at 1 Ryd and spectral slope  $\alpha_b = 1.8$ , as described in § 3.2. (The BL Lac, PKS 2155-304 cannot dominate the ionizing flux incident on these clouds, unless its actual redshift is much less than the value,  $z = 0.116$ , from Falomo et al. 1993.) If  $I_0$  and  $D$  are constant, then  $N(\text{H I}) \propto n_{\text{HI}} \propto n_H^2$ , so that total density,  $n_H$ , and gas mass,  $M_{\text{gas}}$ , scale as  $[N(\text{H I})]^{1/2}$ . For the parameters above, the mean densities are  $\langle n_{\text{HI}} \rangle = 2.2 \times 10^{-8}$

cm<sup>−3</sup> and  $\langle n_{\text{H}} \rangle = 4.4 \times 10^{-5}$  cm<sup>−3</sup>, and the total gaseous mass, including helium, is

$$M_{\text{gas}} = (4 \times 10^{11} M_{\odot}) \left[ \frac{R}{500 \text{ kpc}} \right]^2 \left[ \frac{\text{N(H I)}}{2 \times 10^{16} \text{ cm}^{-2}} \right]^{1/2}. \quad (2)$$

The gas mass could therefore approach 1% of the  $10^{14} M_{\odot}$  required to bind the group, a relatively small gas fraction compared to the gas found in clusters and elliptical-rich groups. Likewise, the luminous mass in these galaxies is small. If the gas is clumped into denser parcels with the same total covering factor, the neutral fraction would increase and the total gas mass would decrease inversely with the characteristic depth of the absorbers.

Let us now consider inhomogeneous models for the gas distribution around PKS 2155-304, involving dwarf galaxies or primordial gas filaments. Let the total projected area of the gas be  $L \times L$  with depth  $D$ , where  $L \approx 1$  Mpc and  $D \approx 400$  kpc. Assume that this volume is filled by an ensemble of  $N_{\text{cl}}$  clouds, each of radius  $r \approx 40$  kpc, with a velocity dispersion 750 km s<sup>−1</sup>. The cloud filling factors in area and volume are,  $f_A = \pi N_{\text{cl}}(r/L)^2$  and  $f_V = (4\pi/3)N_{\text{cl}}(r/L)^3(L/D)$ , where  $f_A$  could exceed 1 if clouds overlapped in projected area. Using the given parameters, their ratio is  $(f_A/f_V) = (4/3)(r/D) \approx 0.13$ . Since we detected many absorbers along the sightline, it is likely that  $f_A \geq 1$ , which suggests that  $f_V \approx 0.3 - 0.5$ . A consequence of this model is that these “clouds” should collide with one other on a crossing time  $t_{\text{cr}} = (0.6 \text{ Mpc})/(750 \text{ km s}^{-1}) < 10^9$  yr. Therefore, if this group is bound, we would expect considerable gas stripping, with the possibility of shocks, hot gas ( $T \approx 5 \times 10^6$  K), and tidal plumes. There is no evidence for these effects, although there has been no search for extended soft X-ray emission or O VI absorption from this region.

If the group of galaxies and clouds is not bound, then this cloud ensemble could either be primordial gas which never participated in galaxy formation or gaseous halos of luminous or dwarf galaxies. Based upon an extensive survey of quasar fields, for which ultraviolet spectra were obtained by the HST Key Project Team, Lanzetta et al. (1995, hereafter L95) identified  $\sim 1/3$  of large equivalent width ( $W_{\lambda} \geq 0.3$  Å) Ly $\alpha$  absorption lines with bright galaxies at impact parameters  $\leq 210h_{75}^{-1}$  kpc away from the sightline. The three strongest close pairs of Ly $\alpha$  clouds in Table 1 would not be resolved into multiple components at the 1 Å resolution of the Key Project spectra. While all three cloud complexes are easily strong enough to be included in the L95 study, none is as close to a bright galaxy as those in the L95 survey:  $300h_{75}^{-1}$  kpc for the 5100 km s<sup>−1</sup> absorber,  $560h_{75}^{-1}$  kpc for the 16,300 km s<sup>−1</sup> absorber, and  $400h_{75}^{-1}$  kpc for the 17,000 km s<sup>−1</sup> absorber. Our H I detection survey in this field (van Gorkom et al. 1996 and § 2.2 herein) reaches depths at least comparable to the L95 survey (0.1–0.3  $L_*$ ). Thus, the bright galaxy halos in this field may be anomalously larger than those found by L95 in other fields, and also substantially larger than expected theoretically (Dove & Shull 1994). However, we strongly suspect that bright galaxy halos cannot account for these clouds.

Are there undetected dwarf galaxies at the Ly $\alpha$  cloud redshifts closer to the PKS 2155-304 sightline? If so, then dwarf-galaxy halos could be responsible for these absorptions as extrapolated

by L95 and others. Chen et al. (1998) found a best-fit Ly $\alpha$  halo size that scales with galaxy luminosity as  $r_h \propto L^{0.35}$ , a somewhat stronger dependence than the  $r_h \propto L^{0.15}$  found for Mg II absorbing halos (Steidel 1995). With the Chen et al. scaling relation, the two weaker absorption complexes (5100 and 16,200 km s $^{-1}$ ) would be consistent with the L95 and Chen et al. observations if any fainter galaxies ( $L \leq 0.1L_*$ ) were found closer to PKS 2155-304 at those redshifts. However, the 17,000 km s $^{-1}$  absorber is so strong that a dwarf galaxy would need to be very close to the sightline to satisfy the Chen et al. halo-size relationship. Specifically, we would require impact parameters  $\rho < 67h_{75}^{-1}$  kpc for  $L \approx 0.1L_*$  and  $\rho < 33h_{75}^{-1}$  kpc for  $L \approx 0.01L_*$ . The only bright galaxy sufficiently near to PKS 2155-304 to satisfy the first condition is galaxy G4 of Falomo et al. (1993), which has  $L \approx 0.2L_*$  and  $\rho \approx 80h_{75}^{-1}$  kpc. However, G4 has  $z = 0.117$ , the same as PKS 2155-304. While there are some closer galaxies, their numbers are modest: 1 – 3 excess galaxies to  $L \leq 0.01L_*$  based on the independent data from Wurtz et al. (1997) and Falomo et al. (1993). The only two galaxies with spectroscopy in hand are galaxies 1 and 2 of Falomo et al. (1993) at  $z = 0.117$ , located 4 arcsec E and 25 arcsec SE of the BL Lac, respectively. At this point, there is no dwarf galaxy candidate for any of these three strong absorption complexes.

Thus, although unlikely, the dwarf-galaxy halo hypothesis remains possible. We detected one faint dwarf ( $M_B \approx -15$ ) at  $565h_{75}^{-1}$  from the PKS 2155-304 sightline, and we may find other faint galaxies at the redshifts of the three strong absorption complexes. However, there is no direct evidence in favor of the dwarf-halo, and the primordial cloud hypothesis must be taken seriously for all three Ly $\alpha$  absorbers.

### 3.2. Metallicity Limits

We can also use our spectra to set limits on the metallicity of the strongest Ly $\alpha$  absorbers. As seen in Figure 1, metal lines should be searched for in three strong absorption systems, corresponding to Ly $\alpha$  lines at  $\lambda_1 = 1281.393$  Å ( $z_1 = 0.054063$ ),  $\lambda_2 = 1284.484$  Å ( $z_2 = 0.056605$ ), and  $\lambda_3 = 1285.097$  Å ( $z_3 = 0.057110$ ). In the limited wavelength range of our GHRS/G160M spectrum, the only expected strong metal line is the Si III  $\lambda 1206.500$  resonance line. No Si III absorption is present at the 1271.73 Å location of system 1. Although we see a hint of Si III absorption at the expected positions [1274.79 Å and 1275.40 Å, see Fig. 1] corresponding to systems 2 and 3, we treat this absorption as *upper limits*. Using the unsmoothed data to detect weak, unresolved features, we obtain a formal  $4\sigma$  error on equivalent width of 23 mÅ (rest-frame 22 mÅ).

To convert the observed Si III/H I to limits on abundances (Si/H), we must make an ionization correction based on photoionization conditions in the absorbers. Appenzeller et al. (1995) claimed to detect weak Ly $\alpha$  absorption with the far-UV spectrograph aboard *ORFEUS*. The Ly $\alpha$  clouds at  $z = 0.054 - 0.057$  were estimated to have a combined column density  $N(\text{H I}) = (2 - 5) \times 10^{16}$  cm $^{-2}$ . We have derived the expected column densities of metal ions by modeling the strong absorbers as slabs with  $N(\text{H I}) = 2 \times 10^{16}$  cm $^{-2}$  and total depth ranging from 5 to

800 kpc, comparable to or less than the offset distance from the nearest galaxies. The slabs are assumed to be illuminated on both sides by an ionizing spectrum with specific intensity at 1 Ryd of  $I_0 = 10^{-23}$  ergs cm $^{-2}$  s $^{-1}$  Hz $^{-1}$  sr $^{-1}$ , consistent with a recent calculation by Shull et al. (1998) that gives  $I_0 = (1.1 \pm 0.5) \times 10^{-23}$ , based on low- $z$  Seyfert galaxies and a new IGM opacity model. The spectral index of the ionizing background is taken as  $\alpha_s = 1.8 \pm 0.1$  (Zheng et al. 1997).

As a “standard model”, we assume a homogeneous slab, of depth 400 kpc and 0.003 solar metallicity. The photoionization equilibrium is computed with the model CLOUDY Version 90.03 (Ferland 1996). The results are given in Table 4. In general, the C III  $\lambda 977$  and C IV  $\lambda 1548$  lines are the best tracers of metals, while Si III  $\lambda 1206$  is a factor of 5–10 weaker, assuming relative solar abundances of  $(\text{Si/H})_\odot = 3.55 \times 10^{-5}$  and  $(\text{C/H})_\odot = 3.63 \times 10^{-4}$  (Grevesse & Anders 1989). However, the C III line lies shortward of the HST band, and its observation must await the launch of the FUSE satellite in early 1999. For unsaturated absorption, the predicted equivalent widths can be written:

$$W_\lambda(\text{C IV}) = (73 \text{ m}\text{\AA}) \left[ \frac{N(\text{H I})}{2 \times 10^{16} \text{ cm}^{-2}} \right] \left[ \frac{[\text{C/H}]}{0.003} \right], \quad (3)$$

$$W_\lambda(\text{Si III}) = (22 \text{ m}\text{\AA}) \left[ \frac{N(\text{H I})}{2 \times 10^{16} \text{ cm}^{-2}} \right] \left[ \frac{[\text{Si/H}]}{0.003} \right]. \quad (4)$$

Following the convention of our earlier Ly $\alpha$  work, we treat “definite absorbers” as those with  $4\sigma$  significance. The observed 23 m $\text{\AA}$  ( $4\sigma$ ) limit on Si III  $\lambda 1206$  (rest equivalent width 22 m $\text{\AA}$ ) corresponds to  $N(\text{Si III}) \leq 1.0 \times 10^{12} \text{ cm}^{-2}$ . If we scale the column density of the strong absorption components to  $N(\text{H I}) = 2 \times 10^{16} \text{ cm}^{-2}$ , the ( $4\sigma$ ) upper limit on metallicity can be written,

$$\left[ \frac{\text{Si}}{\text{H}} \right] \leq (0.003) \left[ \frac{2 \times 10^{16} \text{ cm}^{-2}}{N(\text{H I})} \right] \left( \frac{\text{Si}}{\text{H}} \right)_\odot. \quad (5)$$

Another limit on metallicity comes from C IV  $\lambda 1548.195$ . From their low-resolution (GHRS/G140L) spectrum, Bruhweiler et al. (1993) quote a ( $2\sigma$ ) upper limit of 110 m $\text{\AA}$  for C IV  $\lambda 1548$ . We recalibrated the pre-COSTAR GHRS/G140L spectrum using IRAF/STSDAS/CALHRS with the final calibration files. As before, subexposure coaddition was performed using our own IDL routines, which merge the subexposures by exposure time with photocathode blemishes removed (Fig. 5). We find a  $4\sigma$  limit of  $W_\lambda \leq 134 \text{ m}\text{\AA}$  (127 m $\text{\AA}$  rest frame) or  $N(\text{C IV}) \leq 3 \times 10^{13} \text{ cm}^{-2}$  for a linear curve of growth. This yields a metallicity limit,

$$\left[ \frac{\text{C}}{\text{H}} \right] \leq (0.005) \left[ \frac{2 \times 10^{16} \text{ cm}^{-2}}{N(\text{H I})} \right] \left( \frac{\text{C}}{\text{H}} \right)_\odot. \quad (6)$$

Figures 6 and 7 illustrate how these metallicities depend on the two key parameters of the photoionization models: the mean hydrogen density  $\langle n_H \rangle$  and the spectral slope  $\alpha_b$  of the ionizing background. The observed column density,  $N(\text{H I})$ , and the assumed cloud depth,  $D$ , determine

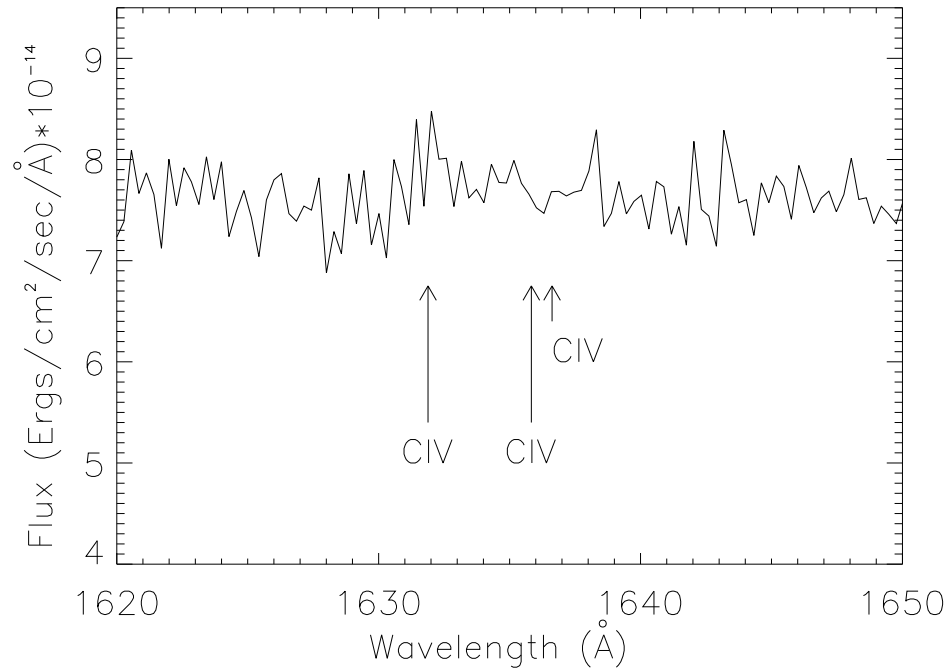


Fig. 5.— GHRS/G140L data of PKS 2155-304 (Bruhweiler et al. 1993) reduced with our software and GHRS final calibration files to show the spectral region for C IV  $\lambda$ 1548.195 absorption corresponding to the three strong Ly $\alpha$  absorbers at 1281.393, 1284.484, and 1285.097  $\text{\AA}$  (see Table 4). The signal-to-noise ratio is 30 per 0.029  $\text{\AA}$  pixel. The C IV upper limits are each 134 m $\text{\AA}$  ( $4\sigma$ ) in the observed frame.

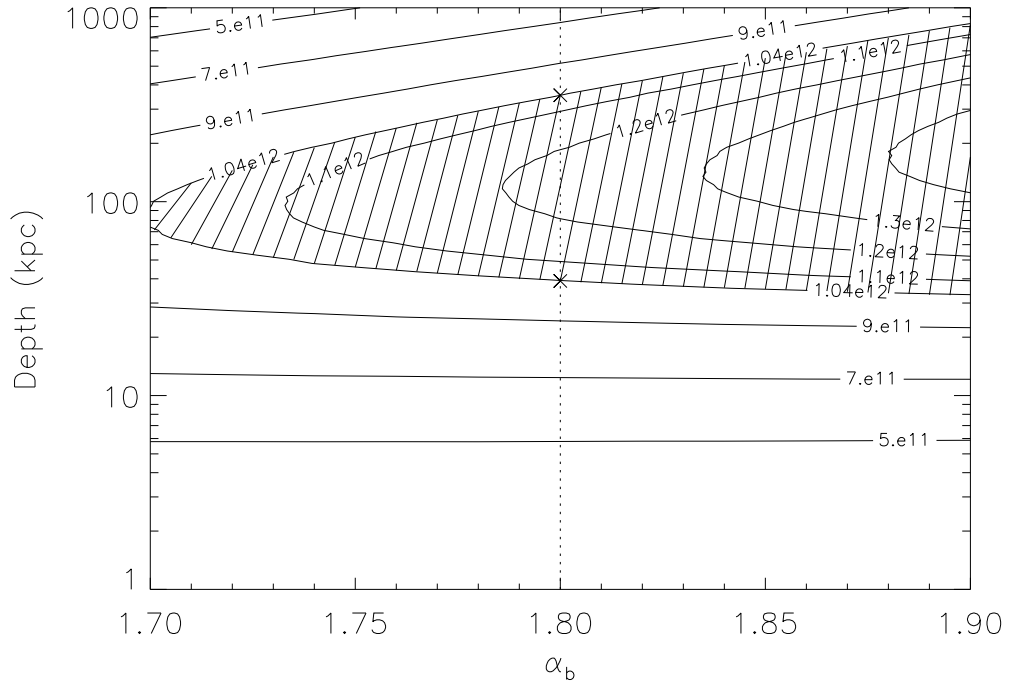


Fig. 6.— Contours of column density,  $N(\text{Si III})$ , corresponding to  $N(\text{H I}) = 2 \times 10^{16} \text{ cm}^{-2}$  and 0.003 solar metallicity. The axes represent the assumed spectral slope of the ionizing background spectra ( $1.7 \leq \alpha_b \leq 1.9$ ) and cloud depths ( $5 \leq D \leq 1000 \text{ kpc}$ ). Hatched lines mark regions disallowed by the  $4\sigma$  non-detection of Si III, while asterisks mark the first viable solutions,  $D \geq 300 \text{ kpc}$  and  $D \leq 40 \text{ kpc}$ , consistent with the standard value  $\alpha_b = 1.8$ . Large- $D$  solutions correspond to absorption from a homogeneous slab, while small- $D$  solutions could arise in denser galactic halos along the sightline.

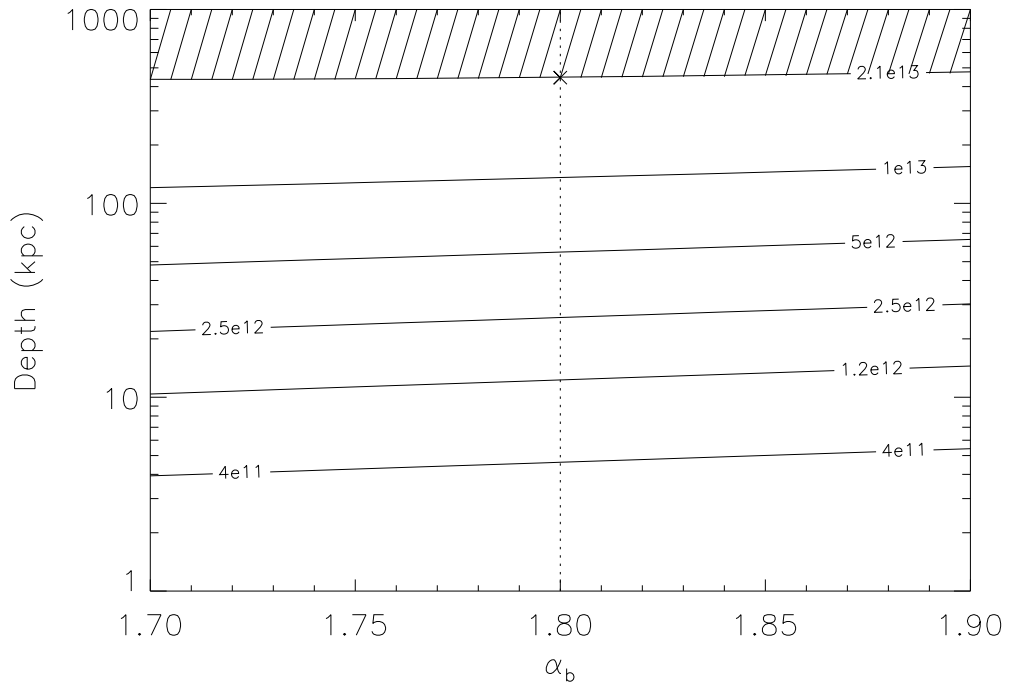


Fig. 7.— Same as Fig. 6, showing contours of column density,  $N(\text{C IV})$ , corresponding to  $N(\text{H I}) = 2 \times 10^{16} \text{ cm}^{-2}$  and 0.003 solar metallicity. Hatched lines mark regions disallowed by the  $4\sigma$  non-detection of C IV, while the asterisk marks the first viable solutions,  $D \leq 400 \text{ kpc}$ , consistent with  $\alpha_b = 1.8$ . Although the combined Si III and C IV limits allow metal-bearing clouds of size 200–400 kpc, there is more parameter space at sizes less than 40 kpc.

the mean neutral density,

$$\langle n_{\text{HI}} \rangle = (1.6 \times 10^{-8} \text{ cm}^{-3}) \left[ \frac{\text{N(H I)}}{2 \times 10^{16} \text{ cm}^{-2}} \right] \left[ \frac{400 \text{ kpc}}{D} \right]. \quad (7)$$

The neutral fraction,  $\langle n_{\text{HI}}/n_H \rangle$ , is set by photoionization equilibrium and is proportional to the ionization parameter,  $U \propto J_0/n_H$ , as are the other metal-ion column densities. The precise behavior of the ratios (Si III/H I) and (C IV/H I) depend on the range of  $U$  where these particular ions peak in fractional abundance (Donahue & Shull 1991). The spectral slope,  $\alpha_b$ , affects the ionization rates above the relevant ionization thresholds (16.34, 33.46, 45.13 eV for Si II, III, IV; 24.38, 47.87, 64.48 eV for C II, III, IV). For a fixed radiation intensity,  $J_0$ , decreasing the assumed cloud depth  $D$  results in a higher  $\langle n_H \rangle$ , smaller ionization parameter  $U$ , larger hydrogen neutral fraction, and lower N(C IV) and N(Si III). For  $\alpha_b = 1.8 \pm 0.1$  and  $D = 400 \pm 200$  kpc, the predicted column densities are:

$$\text{N(Si III)} = (1.0_{-0.2}^{+0.2} \times 10^{12} \text{ cm}^{-2}) \left( \frac{[\text{Si/H}]}{0.003} \right) \quad (8)$$

$$\text{N(C IV)} = (1.8_{-0.5}^{+0.7} \times 10^{13} \text{ cm}^{-2}) \left( \frac{[\text{C/H}]}{0.003} \right). \quad (9)$$

The topology of C IV and Si III differ, as seen in the excluded regions of Figures 6 and 7. For denser absorbers, the ionization equilibrium shifts to lower ionization parameter ( $U$ ) in which case C IV/H I decreases (Fig. 7) while Si III/H I remains about the same (Fig. 5). For Si III, the ionization solutions can be double-valued, since Si III changes more strongly with  $U$  than H I (Donahue & Shull 1991). At sufficiently low and sufficiently high ionization parameter, silicon lies in other states (Si II or Si IV). As a result, the H I absorption toward PKS 2155-304 could still contain metals at 0.01 solar and arising either in a homogeneous slab, of depth  $D = 200\text{--}400$  kpc, or in denser parcels such as 10–40 kpc halos of dwarf galaxies or intergalactic clouds.

Thus, it is easier to hide metals from detection in the C IV lines than in Si III. The observed limit on Si III absorption with  $\text{N(H I)} = 2 \times 10^{16} \text{ cm}^{-2}$  and 0.003 metallicity formally allows solutions with  $D > 400$  kpc or  $D < 40$  kpc. Limits on C IV absorption allow  $D < 400$  kpc. The combined C IV and Si III limits, together with the numerous discrete Ly $\alpha$  absorbers in velocity space, suggest that the gas may be inhomogeneous on scales of tens of kpc. However, it is puzzling how clumped absorbers could maintain a high density contrast when these clumps would be expected to collide on a billion-year time scale. Such collisions would also shock-heat the gas possibly making C IV lines more detectable. Filamentary sheets, with large aspect ratios, provide a more plausible scenario consistent with these constraints.

Before concluding this section, it is worth examining the accuracy of the measurements of  $\text{N(H I)}$ . Our assumed value,  $\text{N(H I)} = 2 \times 10^{16} \text{ cm}^{-2}$ , comes from the claimed detection of a Ly $\alpha$  depression in *ORFEUS* data (Appenzeller et al. 1995). These data suggest a flux discontinuity shortward of 970 Å, corresponding to the  $z = 0.054 - 0.057$  Ly $\alpha$  absorbers, but the Lyman break

is not definitive, owing to the moderate (0.5 Å) spectral resolution, low signal-to-noise (S/N = 15), and uncertainties in defining and extrapolating the true continuum between 920 and 1100 Å. For similar reasons, these data are not sufficiently accurate to determine N(H I) from a curve-of-growth analysis of the higher Lyman series, Ly $\beta$  – Ly $\delta$ .

Because of Ly $\alpha$  line saturation in our HST/GHRS data, we cannot confirm the large H I columns implied by the Lyc absorption. However, we can provide both a firm lower limit and give reasonable estimates from the strongest Ly $\alpha$  features at 1284–1285 Å. The optical depth of the Ly $\alpha$  line per unit velocity is  $\tau(v) = (\pi e^2/m_e c) f \lambda N(v)$ , where  $N(v)$  is the H I column density per unit velocity. We may integrate this, for  $f = 0.4164$  and  $\lambda = 1215.67$  Å, to obtain,

$$N_{\text{tot}} = (7.45 \times 10^{11} \text{ cm}^{-2}) \int \tau(v) dv , \quad (10)$$

where  $v$  is measured in km s $^{-1}$ . In our post-COSTAR data, with S/N  $\approx 20$ , this formula provides only a minimum column density, since we cannot distinguish optical depths  $\tau(v) > 3$ . Flux calibration and background subtraction are difficult with the GHRS one-dimensional detectors. An integration of the data (Fig. 8) yields values  $N_{\text{tot}}$  ranging from  $(3 - 10) \times 10^{14} \text{ cm}^{-2}$ . Values of  $2 \times 10^{16} \text{ cm}^{-2}$  needed for consistency with the *ORFEUS* Lyc measurement would require unresolved narrow components in the line core.

Although we have some skepticism about adopting the  $(2 \times 10^{16} \text{ cm}^{-2})$  column density from *ORFEUS*, it is worth remembering that line saturation and multiple velocity components make column density measurement extremely difficult from just one line. A prime example of this difficulty comes from the Ly $\alpha$  absorbers seen toward 3C 273 at  $cz \sim 1000$  km s $^{-1}$  and  $cz \sim 1600$  km s $^{-1}$  (Weymann et al. 1995). Recent *ORFEUS* measurements of these components (Hurwitz et al. 1998) find Ly $\beta$  absorption equivalent widths larger by factors of 1.5 and 2.4 than values predicted by Ly $\alpha$  Voigt profile fits of HST/GHRS data ( $\log N = 14.19$  and  $b = 40.7$  km s $^{-1}$  for the 1000 km s $^{-1}$  cloud, and  $\log N = 14.22$ ,  $b = 34.2$  km s $^{-1}$  for the 1600 km s $^{-1}$  cloud). By analyzing both Ly $\alpha$  and Ly $\beta$ , Hurwitz et al. (1998) derive a best-fit of  $\log N = 15.8$  and  $b = 17$  km s $^{-1}$ . They conclude that, if the H I absorption arises in a single cloud, its column density is higher by at least a factor of 4 compared to the value of Weymann et al. (1995).

Thus, it could be that the strong, saturated Ly $\alpha$  lines towards PKS 2155-304 have columns well above  $10^{15} \text{ cm}^{-2}$  and even as high as  $2 \times 10^{16} \text{ cm}^{-2}$ . This could arise if narrow H I components are hidden within the line core at  $17,000 \pm 50$  km s $^{-1}$ . For example, 20 components, each with  $b \approx 15$  km s $^{-1}$  and  $N(\text{H I}) \approx 10^{15} \text{ cm}^{-2}$ , spread stochastically over  $\sim 100$  km s $^{-1}$  would reproduce the Ly $\alpha$  and Lyc data. Each component would have central optical depth  $\tau_0 \approx 50$  and an (isolated) equivalent width of 240 mÅ. Saturation and velocity overlap would allow their accumulated Ly $\alpha$  absorption to give the observed  $\sim 0.8$  Å, while the Lyc optical depth could reach values  $\tau_c \approx 0.1$ .

Without better data on the Lyc absorption edges or the higher Lyman series lines, we cannot verify the Ly $\alpha$  absorption ( $2 \times 10^{16} \text{ cm}^{-2}$ ) in the strong absorber at  $cz = 16,970$  km s $^{-1}$ . Confirmation of the Lyman limit and higher Lyman series will await our planned studies of

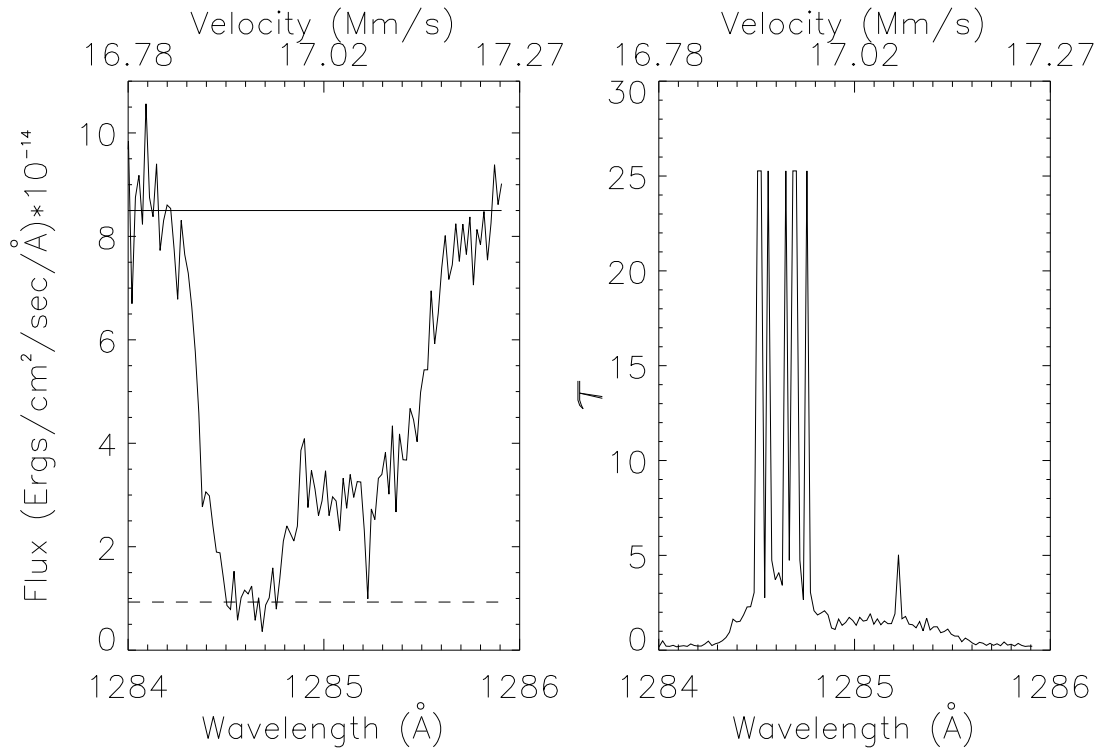


Fig. 8.— Blow-up of the Ly $\alpha$  absorption cluster at  $cz \approx 17,000 \text{ km s}^{-1}$ . Left: Ly $\alpha$  absorption line vs. wavelength and heliocentric velocity,  $cz$ , showing the continuum flux (solid line at top) and  $1\sigma$  background (dashed line at bottom). Right: optical depth,  $\tau(v)$  of the same absorption line, computed from left panel, assuming that the continuum lies at the dashed line. We ignore negative fluxes and values  $\tau > 25$ . Owing to uncertainties in flux calibration and background subtraction, values  $\tau > 3$  are unreliable. The integral of this absorption yields  $N(\text{H I}) = (3 - 10) \times 10^{14} \text{ cm}^{-2}$  (the higher value for right panel shown here). Larger columns, consistent with the *ORFEUS* LyC estimates,  $N(\text{H I}) = (2 - 5) \times 10^{16} \text{ cm}^{-2}$ , would require unresolved narrow components in the line core.

PKS 2155-304 following the scheduled Feb. 1999 launch of the Far Ultraviolet Spectroscopic Explorer (FUSE). With FUSE, if  $N(H I)$  is as large as  $2 \times 10^{16} \text{ cm}^{-2}$ , the Lyman edge at 963.36 Å will have  $\tau_c \approx 0.13$ , and many higher Lyman lines will be detectable. Even if we adopt the minimum values,  $N(H I) \geq 4 \times 10^{14} \text{ cm}^{-2}$  and  $\tau(\text{Ly}\alpha) \geq 3$  in the line core, we should be able to detect higher Lyman lines with  $\tau(\text{Ly}\beta) \geq 0.48$ ,  $\tau(\text{Ly}\gamma) \geq 0.17$ , and  $\tau(\text{Ly}\delta) \geq 0.08$ . It would also be helpful to obtain a better Ly $\alpha$  spectrum of the 1270-1290 Å region with HST/STIS, whose two-dimensional array detectors will improve the background subtraction and flux calibration. The metal-line searches can also be improved with HST, using STIS and COS (see § 3.4).

If  $N(H I)$  is smaller than the value ( $2 \times 10^{16} \text{ cm}^{-2}$ ) assumed in Figures 5 and 6, our limits on metallicity increase. For homogeneous clouds, of constant density, several quantities follow from simple scaling relations of  $N(H I)$ . First, our inferred value of D/H scales inversely with  $N(H I)$ , and would therefore go up. Second, one would find a tradeoff of cloud depth ( $D$ ) and metallicity ([C/H] or [Si/H]). If  $N(H I)$  were decreased by a factor 10, the metallicity limits would rise by the same factor. If  $D$  is held constant, a simple scaling of the metallicity with  $N(H I)$  is not possible. As we discussed earlier, the relative ionization fractions of H I, C IV, and Si III all vary with ionization parameter,  $U$ . If we retain our estimate of the radiation background and assume  $D = 400 \text{ kpc}$ , reducing  $N(H I)$  by a factor of 10 changes the metallicity limits to  $\text{C/H} < 0.023$  and  $\text{Si/H} < 0.14$  times solar. For the range in ionization parameter  $-1.9 < \log U < -1.3$  appropriate to these assumptions about cloud density and radiation field, the greater sensitivity to  $U$  of the Si III fraction causes the Si III constraints on metallicity to weaken much more rapidly with decreasing  $N(H I)$ . Regardless of the exact value of  $N(H I)$ , the most sensitive metal lines remain upper limits. Therefore, one must take seriously the possibility that these clouds are primordial.

### 3.3. Limits on Deuterium

A similar analysis can be done using the strong absorbers to search for weak deuterium Ly $\alpha$  (1215.339 Å) features in the shortward wings of H I Ly $\alpha$  (1215.667 Å). No deuterium feature is seen in the wings of the H I system 1 (H I at 1281.393 Å, D I at 1281.044 Å) to a level of  $W_\lambda \leq 20 \text{ m}\text{\AA}$ . In system 2 (H I at 1284.484 Å, D I at 1284.133 Å) the limit is  $W_\lambda \leq 30 \text{ m}\text{\AA}$ . For a linear curve of growth, these equivalent widths translate to  $N(D I) \leq 3.7 \times 10^{12} \text{ cm}^{-2}$  and  $5.5 \times 10^{12} \text{ cm}^{-2}$ , respectively. If we attribute column densities  $N(H I)$  of  $1 \times 10^{16} \text{ cm}^{-2}$  and  $2 \times 10^{16} \text{ cm}^{-2}$  to systems 1 and 2, respectively, these limits give a deuterium abundance limits of,

$$\left(\frac{D}{H}\right) \leq (3.7 \times 10^{-4}) \left[ \frac{1 \times 10^{16} \text{ cm}^{-2}}{N(H I)} \right] \text{ (system 1)} \quad (11)$$

$$\left(\frac{D}{H}\right) \leq (2.8 \times 10^{-4}) \left[ \frac{2 \times 10^{16} \text{ cm}^{-2}}{N(H I)} \right] \text{ (system 2)} \quad (12)$$

These limits can be improved significantly with higher-precision data on the D I line (with

HST/STIS) and with better H I column densities from higher Lyman-series lines (with the FUSE spectrograph). At the current level of accuracy, neither limit provides a strong constraint on Big Bang nucleosynthesis (Schramm & Turner 1998). The interstellar medium value has been reported in the range  $D/H = (1.6 \pm 0.09) \times 10^{-5}$  (Linsky et al. 1993, 1995). However, a controversy still exists over the high-redshift D/H observed in QSO absorption systems. A recent determination of D/H in two QSO Lyman-limit systems (Burles & Tytler 1997) gives a “low value”,  $D/H = (3.4 \pm 0.25) \times 10^{-5}$ , while Songaila and Cowie (cf. Songaila 1997) quote “high values” with a range  $D/H = (0.4 - 1.5) \times 10^{-4}$ . The high values of D/H would obviously require a large destruction rate of deuterium through star formation. Thus, it would be helpful to obtain a detection of deuterium in the strong Ly $\alpha$  systems at  $z = 0.054 - 0.057$  toward PKS 2155-304. Here, the measured metallicity is much less than solar values, implying little astration of D. We expect that future HST and FUSE observations can make a factor of 3 improvement in sensitivity, which could set a limit on  $D/H < 1 \times 10^{-4}$ .

### 3.4. Future Searches for Metal Absorption

Our photoionization models demonstrate that, for clouds with  $\geq 0.001$  solar metallicity, it should be possible, with better HST/STIS data, to detect the 1548.2 Å and 1550.8 Å resonance lines of C IV. We may also be able to detect C II  $\lambda 1335$ , N V  $\lambda 1238$ , Si IV  $\lambda 1394$ , and Si III  $\lambda 1206$ . With the FUSE satellite, we intend to search for C III  $\lambda 977$ , C II  $\lambda 1036$ , and O VI  $\lambda 1032$ . The C III line should be detectable down to well below 0.001 solar metallicity. The C II lines might be present if the gas is at higher density (lower  $U$ ). The O VI line is weaker in the standard model ( $D = 400$  kpc,  $\alpha_b = 1.8$ ), but it might be enhanced by a number of effects: a hard photoionizing radiation field above 114 eV, a collisionally ionized component due to hot gas, or oxygen abundance enhancement by massive-star nucleosynthesis. We probably will not detect O I  $\lambda 1302$ , which is weak, even at 3% solar metallicity, because the O I abundance is tied by charge exchange to the ratios (H II/H I) and (O II/O).

Because of the O VI ionization correction, the strength of the  $\lambda 1032$  absorption line depends both on the shape of the ionizing spectrum and on the cloud depth. For example, if  $\alpha_b = 1.4$  ( $D = 400$  kpc) the O VI column density increases by over a factor of 4, while if  $\alpha_b = 1.8$  ( $D = 600$  kpc) it increases by a factor of 2. The *total* H I column in the absorbers could be higher than the assumed value,  $2 \times 10^{16}$  cm $^{-2}$ . In addition, the Si and O abundances could be enhanced (Songaila & Cowie 1996; Giroux & Shull 1997) relative to C in regions dominated by “prompt nucleosynthesis” from massive-star supernovae. Thus, if  $\text{Si/C} > 2 \times (\text{Si/C})_{\odot}$  and  $\text{O/C} > 2 \times (\text{O/C})_{\odot}$ , we may be able to detect lines of O VI, Si II, Si III, and Si IV.

As shown by Donahue & Shull (1991), the ratios of column densities from multiple ion states of the same element (e.g., Si II/III/IV and C II/IV) can be modeled to provide diagnostics of the intensity and spectrum of the 1–4 Ryd ionizing radiation field. Detections of these ions would allow us to discriminate between an extragalactic radiation field due to AGN or due to O-stars

from starburst galaxies.

#### 4. CONCLUSIONS

The sightline to PKS 2155-304 is unique among the AGN studied thus far for low-redshift Ly $\alpha$  absorbers. It has the highest frequency of absorbers, and they are identified with a concentration of bright galaxies. The Ly $\alpha$  absorbers at  $cz \approx 17,000$  km s $^{-1}$  may be an extreme example of the previously known association of Ly $\alpha$  clouds with the extended halos of galaxies (Lanzetta et al. 1995; Stocke et al. 1995). Of greater interest is the enormous inferred gaseous extent; the nearest bright galaxies lie  $(400 - 800)h_{75}^{-1}$  off the sightline. These offsets are so large that they are unlikely to represent equilibrium gaseous disks; the orbital times at such distances would be enormous. We have interpreted these absorbers as large sheets of intragroup gas, or as smaller primordial clouds and halos of dwarf galaxies. The clumpiness of the Ly $\alpha$  absorption in velocity space suggests that some spatial structure is present. However, as discussed in § 3.1, a medium that is clumpy in both space and velocity would be subject to disruptive collisions.

Our major conclusions are therefore:

- The metallicity limits for the Ly $\alpha$  absorbers give (Si/H) and (C/H) less than 0.003 solar if  $N(\text{H I}) = 2 \times 10^{16}$  cm $^{-2}$  (the value from ORFEUS). The greatest uncertainty in these metallicities is the precise value of  $N(\text{H I})$ . We will use the FUSE satellite to measure the H I columns through Lyman limit absorption and higher Lyman series lines. We hope to see discrete absorption edges at 961.04, 963.36, and 963.82 Å.
- Our metallicity limit, [Si/H] < 0.003 solar contradicts the hypothesis that these clouds are metal-enriched intragroup gas. Mushotzky & Loewenstein (1997) suggest that intracluster gas might be enriched early (at  $z > 0.4$ ) to levels of 10% solar metallicity. Evidently, the intergalactic gas around PKS 2155-304 has not been enriched to the levels observed in X-ray emitting intracluster gas.
- If the “small group” hypothesis is correct, a search for X-rays with AXAF imagers would test whether any hot gas has been produced by tidal effects or stripping.
- Future spectral observations with HST can provide even better limits on D/H, Si III, and C IV than those reported here. With FUSE, we will be able to search for the expected strong C III  $\lambda 977$  line, the weak O VI  $\lambda 1032$ , as well as absorption lines of S II, C II, S II, and N II which may be present if the absorption occurs in denser halos.
- The low metallicity limits and the large projected distances from the nearest galaxies suggest that these clouds could be primordial.

This work was based on observations with the NASA/ESA *Hubble Space Telescope* obtained at the Space Telescope Science Institute, which is operated by AURA, Inc. under NASA contract NAS5-26555 and on observations made with NRAO's Very Large Array. The NRAO is operated by Associated Universities, Inc. under a cooperative agreement with the National Science Foundation. We thank Michael Fall and Richard Mushotzky for helpful discussions on the evolution of intracluster gas. This work was supported by HST Guest Observer grant GO-06593.01-95A and by the Astrophysical Theory Program (NASA grant NAGW-766 and NSF grant AST96-17073) to the University of Colorado and by an NSF grant (AST96-17177) to Columbia University.

**Table 1**  
**HST Absorption Features<sup>a</sup> in PKS 2155-304**

| Wavelength<br>(Å) | Velocity <sup>b</sup><br>(km s <sup>-1</sup> ) | Rest EW<br>(mÅ) | Significance <sup>c</sup><br>( $\sigma$ ) | ID                       |
|-------------------|--|-----------------|---|--------------------------|
| 1226.362 ± 0.054  | 2637 ± 13                                      | 42 ± 24         | 9.0                                       | Ly $\alpha$              |
| 1226.990 ± 0.062  | 2789 ± 15                                      | 36 ± 18         | 8.0                                       | Ly $\alpha$              |
| 1232.032 ± 0.045  | 4035 ± 11                                      | 21 ± 11         | 4.2                                       | Ly $\alpha$              |
| 1235.941 ± 0.050  | 4999 ± 12                                      | 129 ± 7         | 29  | Ly $\alpha$              |
| 1236.436 ± 0.100  | 5121 ± 24                                      | 201 ± 8         | 45  | Ly $\alpha$              |
| 1238.426 ± 0.099  | 5612 ± 24                                      | 21 ± 10         | 4.8                                       | Ly $\alpha$              |
| 1238.744 ± 0.065  | 5690 ± 16                                      | 85 ± 22         | 20  | Ly $\alpha$              |
| 1239.817 ± 0.040  | Galactic                                       | 33 ± 12         | 7.5                                       | Mg II                    |
| 1240.411 ± 0.052  | Galactic                                       | 20 ± 11         | 4.5                                       | Mg II                    |
| 1250.588 ± 0.015  | Galactic                                       | 80 ± 11         | 19  | S II                     |
| 1253.807 ± 0.011  | Galactic                                       | 127 ± 12        | 28  | S II                     |
| 1259.519 ± 0.007  | Galactic                                       | 132 ± 16        | 15  | S II                     |
| 1259.869 ± 0.019  | Galactic                                       | 75 ± 20         | 8.8                                       | Si II (HVC) <sup>d</sup> |
| 1260.398 ± 0.055  | Galactic                                       | 467 ± 81        | 53  | Si II+Fe II              |
| 1270.802 ± 0.014  | 13,596 ± 4                                     | 102 ± 17        | 12  | Ly $\alpha$              |
| 1281.393 ± 0.006  | 16,208 ± 2                                     | 345 ± 22        | 45  | Ly $\alpha$              |
| 1281.867 ± 0.063  | 16,325 ± 16                                    | 68 ± 30         | 9.2                                       | Ly $\alpha$              |
| 1284.484 ± 0.009  | 16,970 ± 2                                     | 448 ± 22        | 61  | Ly $\alpha$              |
| 1285.097 ± 0.013  | 17,121 ± 3                                     | 363 ± 24        | 48  | Ly $\alpha$              |
| 1287.515 ± 0.010  | 17,717 ± 3                                     | 141 ± 16        | 19  | Ly $\alpha$              |
| 1288.976 ± 0.020  | 18,078 ± 5                                     | 100 ± 19        | 13  | Ly $\alpha$              |

<sup>a</sup> Top group of lines measured from previously unpublished, pre-COSTAR GHRS/G160M spectrum (Fig. 2). Bottom group is from our post-COSTAR, GHRS/G160M spectrum (Fig. 1). We use global continuum fits and quote rest-frame equivalent widths (EW).

<sup>b</sup> LSR velocity ( $cz$ ), which is the same as heliocentric velocity for this sightline to within  $\pm 1$  km s<sup>-1</sup>. Wavelength scales have been aligned assuming that the Galactic S II lines lie at  $V_{\text{LSR}}$ . This procedure gives offsets of +0.029 Å (new data) and -0.001 Å (pre-COSTAR data).

<sup>c</sup> Significance of the line (in  $\sigma$ ) is defined as the integrated S/N per resolution element of the fitted absorption feature.

<sup>d</sup> High velocity cloud was detected in C IV at  $V_{\text{LSR}} = -141 \pm 9$  km s<sup>-1</sup> (Sembach et al. 1998).

**Table 2**  
**VLA Instrumental Parameters**

|  |                      |
|--|----------------------|
| Date   | 1996 May             |
| Configuration                                      | DnC                  |
| Integration time (hrs)                             | 40                   |
| Central Velocity (km s <sup>-1</sup> )             | 16,880               |
| Channel Width (kHz)                                | 195                  |
| Channels   | 31                   |
| Velocity Resolution (km s <sup>-1</sup> )          | 46                   |
| Usable Velocity Range (km s <sup>-1</sup> )        | 16,283 - 17,571      |
| Synthesized beam (arcsec)                          | 54.4 × 36.6          |
| rms noise (mJy/beam)                               | 0.15                 |
| rms column density sensitivity (cm <sup>-2</sup> ) | 4 × 10 <sup>18</sup> |

**Table 3**  
**H I Properties of Detected Galaxies**

| Name               | RA (1950)  | Dec (1950)  | $V_{\text{hel}}$<br>(km s <sup>-1</sup> ) | Velocity Range<br>(km s <sup>-1</sup> ) | $M_{\text{HI}}$<br>(10 <sup>9</sup> $M_{\odot}$ ) | $L_B/L_*$ |
|--------------------|------------|-------------|---|---|---|-----------|
| 2155-3033          | 21 55 46.9 | -30 33 49.6 | 17,087                                    | 16,888 - 17,294                         | 7.4   | 1.4       |
| F21569-3030        | 21 56 56.0 | -30 30 43.7 | 16,785                                    | 16,650 - 16,926                         | 14  | 0.9       |
| uncataloged        | 21 56 03.6 | -30 17 08.7 | 17,179                                    | 17,064 - 17,294                         | 4.9   | 0.3       |
| APMBGC 466-053+024 | 21 55 29.9 | -30 33 52.6 | ~ 16,200                                  | < 16,237 - 16,375                       | > 3.6   | 3.0       |
| uncataloged        | 21 56 38.5 | -30 30 57.4 | 17,156                                    | 17,156                                  | 0.8   | 0.014     |

**Table 4**  
**Predicted Column Densities<sup>a</sup> and Equivalent Widths**

| Ion    | Column Density<br>(cm <sup>-2</sup> ) | $W_\lambda$<br>(mÅ) | $\lambda_0$<br>(Å) | Observed $\lambda_i$<br>[ $\lambda_0(1 + z_i)$ ] |
|--------|---------------------------------------|---------------------|--------------------|--|
| C II   | $1.1 \times 10^{12}$                  | 2.2                 | 1334.532           | 1406.68, 1410.07, 1410.75                        |
| C III  | $2.4 \times 10^{13}$                  | 156                 | 977.020            | 1029.84, 1032.32, 1032.82                        |
| C IV   | $1.8 \times 10^{13}$                  | 73                  | 1548.195           | 1631.90, 1635.83, 1636.61                        |
| N V    | $1.7 \times 10^{12}$                  | 3.6                 | 1238.821           | 1305.80, 1308.94, 1309.57                        |
| O VI   | $1.6 \times 10^{12}$                  | 2.0                 | 1031.926           | 1087.72, 1090.34, 1090.86                        |
| Si II  | $6.5 \times 10^{10}$                  | 1.0                 | 1260.422           | 1328.56, 1331.77, 1332.40                        |
| Si III | $1.0 \times 10^{12}$                  | 22                  | 1206.500           | 1271.73, 1274.79, 1275.40                        |
| Si IV  | $5.8 \times 10^{11}$                  | 4.5                 | 1393.755           | 1469.11, 1472.65, 1473.35                        |

<sup>a</sup> Column densities are computed for cloud with  $N_{\text{HI}} = 2 \times 10^{16}$  cm<sup>-2</sup>,  $D = 400$  kpc, and 0.003 solar metallicity, irradiated by QSO ionizing spectrum with  $\alpha_b = 1.8$  and  $I_0 = 10^{-23}$  ergs cm<sup>-2</sup> s<sup>-1</sup> Hz<sup>-1</sup> sr<sup>-1</sup>. Observed wavelengths correspond to Ly $\alpha$  components at 1281.393, 1284.484, and 1285.097 Å, at redshifts  $z_1 = 0.054063$ ,  $z_2 = 0.056605$ , and  $z_3 = 0.057110$ . Equivalent widths are quoted in the rest frame.

## REFERENCES

Allen, R. G., Smith, P. S., Angel, J. R. P., Miller, B. W., Anderson, S. F., & Margon, B. 1993, *ApJ*, 403, 610

Appenzeller, I., Mandel, H., Krautter, J., Bowyer, S., Hurwitz, M., Grewing, M., Kramer, G., & Kappelmann, N. 1995, *ApJ*, 439, L33

Bahcall, J. N. et al. 1991, *ApJ*, 377, L5

Bruhweiler, F. C., Boggess, A., Norman, D. J., Grady, C. A., Urry, C. M., & Kondo, Y. 1993, *ApJ*, 409, 199

Burles, S., & Tytler, D. 1997, preprint (astro-ph/9712265)

Canizares, C. R., & Kruper, J. 1984, *ApJ*, 278, L99

Cen, R., Miralda-Escudé, J., Ostriker, J. P., & Rauch, M. 1994, *ApJ*, 437, L9

Chen, H.-W., Lanzetta, K. M., Webb, J. K., & Barcons, X. 1998, *ApJ*, 498, 77

Cowie, L. L., Songaila, A., Kim, T.-S., & Hu, E. M. 1995, *AJ*, 109, 1522

Donahue, M., & Shull, J. M. 1991, *ApJ*, 383, 511

Dove, J. B., & Shull, J. M. 1994, *ApJ*, 423, 196

Falomo, R., Pesce, J. E., & Treves, A. 1993, *ApJ*, 411, L63

Ferland, G. 1996, Hazy, University of Kentucky Internal Report (Version 90.03)

Giroux, M. L., & Shull, J. M. 1997, *AJ*, 113, 1505

Grevesse, N., & Anders, E. 1989, in *Cosmic Abundances of Matter*, AIP Conf. 183, ed. C. J. Waddington, 1.

Grogin, N. A., & Geller, M. J. 1998, *ApJ*, in press (astro-ph/9804326)

Hernquist, L., Katz, N., Weinberg, D. H., & Miralda-Escudé, J. 1996, *ApJ*, 457, L51

Hurwitz, M., et al. 1998, *ApJ*, 500, L61

Lauberts, F., & Valentijn, E. A. 1989, *The Surface Photometry Catalog of the ESO-Uppsala Galaxies*, (Garching, ESO)

Linsky, J. L., et al. 1993, *ApJ*, 402, 694

Linsky, J. L., et al. 1995, *ApJ*, 451, L335

Loveday, J. 1996, *MNRAS*, 278, 1025

Madejski, G., et al. 1998, preprint, submitted to *ApJ*

Maraschi, L., Blades, J. C., Calanchi, C., Tanzi, E. G., & Treves, A. 1988, *ApJ*, 333, 660

Marzke, R. O., Huchra, J. P., & Geller, M. J. 1994, *ApJ*, 428, 43

Morris, S., Weymann, R. J., Savage, B., & Gilliland, R. L. 1991, *ApJ*, 377, L21

Morris, S., Weymann, R. J., Dressler, A., McCarthy, P. J., Smith, B. A., Terrile, R. J., Giovanelli, R., & Irwin, M. 1993, *ApJ*, 419, 524

Mulchaey, J. S., & Zabludoff, A. I. 1998, *ApJ*, 496, 73

Mushotzky, R., & Loewenstein, M. 1997, *ApJ*, 481, L63

Penton, S., Shull, J. M., & Edelson, R. 1998, Database of IUE-AGN Ultraviolet Spectra, available on Website (<http://casa.colorado.edu/~spenton/IUEAGN/FUSE.html>)

Penton, S., Stocke, J. T., & Shull, J. M. 1998, in preparation.

Sandage, A. 1975, in *Galaxies and the Universe*, ed. by A. Sandage, M. Sandage, J. Kristian (University of Chicago Press, Chicago).

Schramm, D. N., & Turner, M. 1998, *Rev. Mod. Phys.*, 70, 303

Sembach, K. R., Savage, B. D., Lu, L., & Murphy, E. M. 1998, *ApJ*, in press

Sherbert, L. E., & Hulbert, S. J. 1997, GHRS Instrument Science Report 067, Official Update (July 1997)

Shull, J. M. 1997, in *Structure and Evolution of the IGM from QSO Absorption Lines*, ed. P. Petitjean & S. Charlot, (Paris, Editions Frontières), 101

Shull, J. M., Stocke, J. T., & Penton, S. 1996, *AJ*, 111, 72

Shull, J. M., Roberts, D., Giroux, M., & Penton, S. 1998, in preparation.

Songaila, A. A. 1997, in *Structure and Evolution of the IGM from QSO Absorption Lines*, ed. P. Petitjean & S. Charlot, (Paris, Editions Frontières), 339

Songaila, A., & Cowie, L. L. 1996, *AJ*, 112, 335

Stark, A. A., Gammie, C. F., Wilson, R. W., Bally, J., Linke, R. A., Heiles, C., & Hurwitz, M. 1992, *ApJS*, 79, 77

Steidel, C. C., 1995, in *QSO Absorption Lines*, Proc. of ESO Symposium, ed. G. Meylan (Heidelberg, Springer), 139

Stocke, J., Shull, J. M., Penton, S., Donahue, M., & Carilli, C. 1995, *ApJ*, 451, 24

Tytler, D. 1995, in *QSO Absorption Lines*, Proc. of ESO Symposium, ed. G. Meylan (Heidelberg, Springer), 289

van Gorkom, J. H. 1993, in *The Environment and Evolution of Galaxies*, ed. J. M. Shull & H. A. Thronson, (Dordrecht, Kluwer), 345

van Gorkom, J. H., Carilli, C. L., Stocke, J. T., Perlman, E. S., & Shull, J. M. 1996, *AJ*, 112, 1397

Weymann, R. J., Rauch, M., Williams, R., Morris, S., & Heap, S. 1995, *ApJ*, 438, 650

Wurtz, R., Stocke, J. T., Ellingson, E., & Yee, H. K. C. 1997, *ApJ*, 480, 547

Zabludoff, A. I., & Mulchaey, J. S., 1998, *ApJ*, 496, 39

Zheng, W., Kriss, G. A., Telfer, R. C., Grimes, J. P., & Davidsen, A. F. 1997, ApJ, 475, 469